

Constraining the Barbero-Immirzi parameter from the duration of inflation in loop quantum cosmology

L. N. Barboza,^{1,*} G. L. L. W. Levy,^{2,†} L. L. Graef,^{1,‡} and Rudnei O. Ramos^{2,§}

¹*Instituto de Física, Universidade Federal Fluminense,*

Avenida General Milton Tavares de Souza s/n, Gragoatá, 24210-346 Niterói, Rio de Janeiro, Brazil

²*Departamento de Física Teórica, Universidade do Estado do Rio de Janeiro, 20550-013 Rio de Janeiro, RJ, Brazil*

We revisit the predictions for the duration of the inflationary phase after the bounce in loop quantum cosmology. We present our analysis for different classes of inflationary potentials that include the monomial power-law chaotic type of potentials, the Starobinsky and the Higgs-like symmetry breaking potential with different values for the vacuum expectation value. Our setup can easily be extended to other forms of primordial potentials than the ones we have considered. Independently on the details of the contracting phase, if the dynamics starts sufficiently in the far past, the kinetic energy will come to dominate at the bounce, uniquely determining the amplitude of the inflaton at this moment. This will be the initial condition for the further evolution that will provide us with results for the number of e -folds from the bounce to the beginning of the accelerated inflationary regime and the subsequent duration of inflation. We also discuss under which conditions each model considered could lead to observable signatures on the spectrum of the cosmic microwave background or else be excluded for not predicting a sufficient amount of accelerated expansion. A first analysis is performed considering the standard value for the Barbero-Immirzi parameter, $\gamma \simeq 0.2375$, which is obtained from black hole entropy calculations. In a second analysis, we consider the possibility of varying the value of this parameter, which is motivated by the fact that the Barbero-Immirzi parameter can be considered a free parameter of the underlying quantum theory in the context of loop quantum gravity. From this analysis, we obtain a lower limit for this parameter by requiring the minimum amount of inflationary expansion that makes the model consistent with the cosmic microwave background observations. When constraining the Barbero-Immirzi parameter, we have made use of the results for the scalar of curvature perturbations derived in loop quantum cosmology assuming the dressed metric approach and considering the Bunch-Davies vacuum as the initial condition for the perturbations in the contracting phase. Such choice provides basically the same results as considering the fourth-order adiabatic vacuum state at the bounce as an initial condition in the context of the dressed metric approach.

I. INTRODUCTION

Inflation is the most popular paradigm for early universe cosmology, but it is not the only one. Indeed, it has been extremely successful from a phenomenological point of view. It predicted the spatial flatness of the Universe, the homogeneity seen in the cosmic microwave background (CMB), besides suggesting a causal explanation for the origin of its anisotropies, providing the first theory for the origin of the large-scale structure of the Universe based on fundamental physics. Although requiring a certain amount of fine-tuning on its constants [1–3] the inflationary scenario predicts correctly the primordial power spectra, whose evolution determines the temperature fluctuations in the CMB and the formation of the large-scale structure of the Universe [2, 4], having been developed before most of the data we now have was on hand.

However, despite the success of inflation, in the classical theory of general relativity (GR), all scalar field models of inflation experience the big bang singularity that

is inevitable [5, 6]. The singularity problem is the result of an extrapolation of GR beyond the limits where the theory is well justified. This implies additional difficulties in the definition of initial conditions due to the absence of a regular surface where those initial conditions can be established. Another related problem in the context of inflation in GR is the fact that there is a very limited value for the number of inflationary e -folds which makes the model theoretically consistent. We know that in order to be compatible with observations, the number of e -folds during inflation should be at least 60 or so. Meanwhile, in some cases, the predicted number of e -folds is more than 70 [7]. In those cases, the scale of the fluctuations which are today observed in the CMB was smaller than the Planck length at the starting of inflation. As a result, the usual semiclassical treatment during inflation is questionable, which is known as the trans-Planckian problem [8, 9]. These issues with the consistency of inflation also motivate to consider scenarios with a well-defined preinflationary dynamics, free of singularities [10–12]. In these scenarios, cosmological perturbations may reach the beginning of inflation in a quantum state excited relative to the Bunch-Davies (BD) vacuum, affecting the power spectra, thus potentially leaving marks on the CMB [13]. In order to address these important issues, one must consider a scenario of quantum gravity acting in the high energy regime. The

* lauziene.barboza@gmail.com

† guslevy9@hotmail.com

‡ leilagraef@id.uff.br

§ rudnei@uerj.br

scenario we consider here lies in the context of loop quantum gravity (LQG).

LQG proposes a quantization formalism based on a nonperturbative and background-independent formulation of the geometric degrees of freedom [14–20]. In its canonical formulation, it is aimed to respect the general covariance of Einstein’s theory. In particular, in GR the Hamiltonian is a linear combination of constraints which, via Poisson brackets, generates diffeomorphism transformations, the fundamental symmetry of the theory [21]. LQG, on the other hand, adopts the quantization scheme proposed by Dirac for systems with constraints, which consists in requiring that those constraints are satisfied at the quantum level on the physical states of the system. The geometric degrees of freedom are described in LQG by pairs of canonical variables, the Ashtekar variables, which consist of the components of a densitized triad and a gauge connection. The quantization is obtained through holonomies of the connections and fluxes of the densitized triads.

Loop quantum cosmology (LQC) is the symmetry reduced version of LQG [18], applied to cosmological models [16, 17, 22]. Taking into account such quantum geometric effects described by LQG in cosmological scenarios, Einstein’s equations maintain an excellent degree of approximation in the low curvature regime. However, in the Planck regime they undergo major changes, driving a nonsingular bounce due to repulsive quantum geometry effects [14, 20], then naturally solving the big bang singularity problem. Therefore, in the LQC framework, for matter satisfying the usual energy conditions, whenever a curvature invariant grows near the Planck scale in LQC, the effects of quantum geometry dilute it [14].

In LQC models with a kinetic energy dominated bounce, as the ones we are going to consider, an inflationary phase almost inevitably follows the bounce phase (see, e.g., Refs. [10, 11, 23–26]). This is true whenever there is an inflaton field, with an appropriate potential, coupled to the gravitational field (otherwise, if there is only radiation and/or cold dark matter in the bounce this does not happen). The duration of this inflationary phase is quantified by the number of e -folds [27–30]. As it is well known [31], the inflationary phase must last at least around 60 e -folds or so in order to solve the problems of the standard cosmological model. However, in LQC, as shown in Ref. [32], the bounce and preinflationary dynamics leaves imprints on the spectrum of the CMB. In Ref. [10] it was shown that, in order to be consistent with observations, the Universe in LQC must have expanded at least around 141 e -folds from the bounce until today. This is so because LQC can lead to scale-dependent features in the CMB spectrum, and the fact that we do not observe them today means that they must have been well diluted by the postbounce expansion of the Universe. This implies an extra number of inflationary e -folds in LQC, given by $\delta N \sim 21$ [10]. On the other hand, if the number of extra inflationary e -folds is much higher than this value the features imprinted in the CMB spectrum

due to the LQC effects would be overly diluted and, in this case, LQC cannot be directly tested even by forthcoming experiments.

Such theoretical results motivate an investigation of the number of e -folds in models of LQC. This can be performed consistently with initial conditions defined either in the bounce, as done, e.g., in Refs. [10, 33], or in a contraction phase before the bounce, as considered in Refs. [34–37], for example; in particular, with the authors of the latter references claiming that taking initial conditions in the far past in the contracting phase should be the appropriate approach to study the probability of inflation after the bounce. Both approaches for choosing the initial conditions to investigate the probability of inflation in LQC were applied to many different potentials. For instance, power-law potentials were considered in Refs. [11, 30, 34–38], alpha-attractor potentials in Ref. [26], monodromy potentials with a modulation term in Ref. [24] and also chaotic and Starobinsky potentials in the framework of standard and modified LQC models [25]. In particular, in the work of Refs. [29, 30], in addition of considering different classes of potentials, the effect of radiation as an additional ingredient of the energy density budget around the bounce has been considered, showing that the duration of inflation is dependent not only on the inflaton potential but also on the amount of radiation in the Universe prior to the start of the inflationary regime.

In the present paper, we show that there are well-defined values for the inflaton amplitude at the bounce, which can be estimated analytically and depending only on the form of the primordial inflaton potential. Then, we provide explicit results, also analytically, for the duration of the preinflationary phase and for the inflaton amplitude at the beginning of the inflationary regime. This then allows us to explicitly obtain the total number of e -folds that inflation will have. Our results are sufficiently general such that it can easily be extended to many different forms of the primordial inflaton potential other than the ones we have focused in this paper.

In the analysis we perform in the first part of this paper, we consider the standard value for the *Barbero-Immirzi parameter*, γ , which is the one arising from the calculation of the entropy of black holes [39]. Then in the second part, we consider the Barbero-Immirzi parameter as a free variable of the theory, and we obtain its value by demanding each model to predict the correct spectrum of CMB. The choice of varying this parameter is motivated by the fact that the Barbero-Immirzi parameter is, indeed, a coupling constant with a topological term in the action of gravity, with no consequence on the classical equations of motion.¹ Although the recovery of the Bekenstein-Hawking entropy has been considered as a way to fix its value, the dependence of the entropy calculation on γ is controversial, and the value $\gamma \simeq 0.2375$

¹ For further discussion in this topic, see, e.g., Refs. [40–49].

calculated thermodynamically is not universally accepted (see, for example, Refs. [50–52]). One can argue that the semiclassical thermodynamical properties can actually be recovered for any value of γ if one makes the appropriated assumptions. When introducing the notion of the horizon into the quantum theory, it was shown that the entropy of large black holes is independent of this parameter and, as it was believed, it is only quantum gravity corrections to the entropy and temperature of small black holes that depend on the Barbero-Immirzi parameter.

When treating γ as a free parameter of the theory, it is important to find ways to constraint its value from observations, if possible. The appearance of this parameter in the area and volume spectra in LQG shows that it plays a role in determining the fundamental length scale of space, since this parameter is used to count the size of the quantum of area in Planck units. If one could resolve distances of around the Planck length, one would be able to fix the Barbero-Immirzi parameter via experiment. Once again, cosmology seems to be a window of opportunity to access such scales, which are unreachable by any terrestrial experiments. As previously discussed, the quantum bounce changes the scalar power spectrum by a correction term which depends on the characteristic scale at the bounce. The characteristic scale is the shortest scale (or largest wave number, namely k_B) that feels the spacetime curvature during the bounce. Since this characteristic scale is dependent on the value of the Barbero-Immirzi parameter, we have a unique opportunity to constrain γ through the observational limits on k_B itself.

In previous works (see, for instance, Refs. [10, 53]), precise constraints on the correction term in the power spectrum of LQC was obtained using the recent CMB data. This observational analysis provided constraints on the characteristic scale k_B . This scale is a function of the Barbero-Immirzi parameter and of the number of e -folds of expansion from the bounce until today. The suggestion of considering the Barbero-Immirzi parameter as a free quantity was in fact first considered in Ref. [34]. In the present paper, we, however, push that idea much further by taking advantage of our analysis and results obtained in the first part of this paper. Then, by using the observational constraints on k_B , we also study their dependence on the Barbero-Immirzi parameter. This will allow us to impose some precise limits on the value of γ as a function of the e -folding number (or equivalently, to obtain constraints on the e -folds number as a function of γ) depending on the primordial inflaton potential.

In summary, in this paper we keep investigating the intriguing possibility that the quantum regime of the Universe in the context of LQC could leave observable signals on CMB, going beyond earlier works in at least two important aspects: (a) First, we investigate the duration of inflation for different potentials including the Starobinsky and Higgs-like potential in addition to the monomial ones, considering that the initial conditions are uniquely determined at the bounce and once we trace the dynamics

far back in the contracting phase. However, our methods are general enough to be able to be extended to other forms of primordial potentials. For practical purposes, we obtain the quantities at some point in the contracting phase and where the kinetic energy of the inflaton starts to dominate over that from the potential. From that point on, we can forward the evolution up to the end of the accelerated inflationary regime; (b) second, we consider the *Barbero-Immirzi parameter* as a free variable of the theory. From our analysis, we then obtain, for the first time, a lower limit for this parameter by requiring the model to be consistent with the CMB observations. We have found constraints on the Barbero-Immirzi parameter in the context of the dressed metric approach and considering the BD vacuum as the initial condition for the perturbations in the contracting phase. Such choice provides basically the same results as considering the fourth-order adiabatic vacuum state at the bounce as the initial condition in the context of the dressed metric approach (for more details, see, for instance, Ref. [10]). Finally, we note that although some monomial potentials are already ruled out in the simple scenarios of cold inflation according to the Planck results, when radiation processes are present (most notably as is the case for these models when studied in the warm inflation context) all of these potentials can be shown to agree with the observations (see, e.g., Refs. [53, 54]). Another reason for analyzing those models here is that they are well motivated in the context of particle physics models in general.

This paper is organized as follows. In Sec. II, we briefly present the main equations of LQC, and also introduce the potentials that we are going to consider in our analysis. In Sec. IIIB, we describe the method used in our analysis and we also establish the way that the initial conditions can be determined and that we are going to use in obtaining the subsequent background dynamical evolution up to the end of inflation. In Sec. IV, we present the results obtained for the duration of inflation in each model considered. The analytical results obtained here are also compared with the numerical results obtained from previous statistical analysis derived in Ref. [30] and in other references. In Sec. V, we discuss the constraints on the value of the Barbero-Immirzi parameter from the required number of inflationary e -folds in each model. In Sec. VI we give our conclusions. One Appendix is included to show some technical details.

II. THEORETICAL BASIS

In this section we briefly introduce the main equations of LQC and we also present the models we are going to consider in this paper.

As discussed in Ref. [33], in LQC the spatial geometry is described by the variable ν proportional to the physical volume of a fiducial cubical cell, in place of the scale

factor a , i.e.,

$$\nu = -\frac{\mathcal{V}_0 a^3 m_{\text{Pl}}^2}{2\pi\gamma}, \quad (2.1)$$

where \mathcal{V}_0 is the comoving volume of the fiducial cell, $m_{\text{Pl}} \equiv 1/\sqrt{G} = 1.22 \times 10^{19}$ GeV is the Planck mass, with G the Newton's gravitational constant and γ is the Barbero-Immirzi parameter. Although γ is actually a free parameter of the theory, in the first part of our work we are going to consider the value motivated from the calculation of the black hole entropy in LQG, which is $\gamma \simeq 0.2375$ [55], which is the value considered in some other studies [50, 51].

The Friedmann equation in LQC assumes the form [33]

$$\frac{1}{9} \left(\frac{\dot{\nu}}{\nu} \right)^2 \equiv H^2 = \frac{8\pi}{3m_{\text{Pl}}^2} \rho \left(1 - \frac{\rho}{\rho_{cr}} \right), \quad (2.2)$$

where

$$\rho_{cr} = \frac{\sqrt{3}m_{\text{Pl}}^4}{32\pi^2\gamma^3} \quad (2.3)$$

is the critical density. Through the modified Friedmann equation (2.2), we see explicitly the underlying quantum geometric effects [14], leading to a bounce in replacement of the singularity when $\rho = \rho_{cr}$. For $\rho \ll \rho_{cr}$ we recover GR as expected.

The energy density ρ in Eq. (2.2) respects the usual conservation equation,

$$\dot{\rho} + 3H(\rho + p) = 0, \quad (2.4)$$

where p is the pressure density.

In models of a single scalar field ϕ with a potential $V(\phi)$, in the Friedmann-Lemaître-Robertson-Walker (FLRW) background, the effective equation of motion for ϕ , the inflaton, is simply

$$\ddot{\phi} + 3H\dot{\phi} + V_{,\phi} = 0, \quad (2.5)$$

where $V_{,\phi} \equiv dV(\phi)/d\phi$ is the derivative of the inflaton's potential.

In the following, we are going to present the models we are going to consider.

A. Models

The classes of inflationary models we are going to consider are described by the potentials below.

1. Power-law monomial potentials

In this class of models, the potential is given by

$$V = \frac{V_0}{2n} \left(\frac{\phi}{m_{\text{Pl}}} \right)^{2n}, \quad (2.6)$$

where n is some power. In this paper we will compare our results with available ones for the cases for the quadratic, quartic and sextic forms of the potential (corresponding to the powers $n = 1, 2$ and 3 , respectively). The model given by Eq. (2.6) covers the class of inflationary models corresponding to large-field models [56].

The new data release from BICEP/Keck [57] strengthened the bounds on the tensor-to-scalar ratio r , putting severe constraints in the full class of monomial potentials, showing that they are disfavored in the context of standard inflation. However, these potentials, besides being well motivated from a particle physics point of view, can still be perfectly allowed in other frameworks, like in the context of warm inflation for example (see, e.g., Ref. [54] and references therein). Since our current analysis can be extended to such frameworks, we consider it important to address this class of potentials here.

2. The Higgs-like symmetry breaking potential

The Higgs-like symmetry breaking potential is given by the following expression,

$$V = \frac{V_0}{4m_{\text{Pl}}^4} (\phi^2 - v^2)^2, \quad (2.7)$$

where v denotes the vacuum expectation value (VEV) of the field. The Higgs-like symmetry breaking potential is another well motivated model from particle physics. Besides that, it can represent either a small-field inflation model, if inflation starts (and ends) at the small field part of the potential (i.e., for $|\phi| < |v|$), or be a large field model, if inflation happens in the large field region of the potential ($|\phi| > |v|$). In all our analyses with this potential, we have explicitly distinguished these two possibilities and produced results for both of them and by also considering different values for the VEV v .

3. The Starobinsky potential

The Starobinsky model [58] is an example of a limiting case of more general modified gravity theories. When expressed in the Einstein frame, it represents a potential which can be written as

$$V = V_0 \left(1 - e^{-\sqrt{\frac{16\pi}{3}} \frac{\phi}{m_{\text{Pl}}}} \right)^2. \quad (2.8)$$

The inflation results derived from the model Eq. (2.8) agree quite well with the observational data for the tensor-to-scalar ratio and spectral tilt [4]. For that reason, it is a popular form of potential in inflation studies.

Note that in Eqs. (2.6) (2.8), the scale V_0 is fixed differently depending on the potential. Its value is determined by the amplitude of the CMB scalar spectrum. Details about its evaluation for the three forms of potentials considered here are giving in the Appendix for completeness.

III. BACKGROUND DYNAMICS IN LQC

The dynamics in the LQC models considered here is assumed to start in the contracting phase sufficiently before the bounce and as originally assumed to be the appropriate moment for setting the initial conditions [34]. Assuming that the initial conditions are set in the contracting phase, when the inflaton field is in the oscillating regime, then, considering a generic inflaton potential of the form $V \propto \phi^m$, $m > 0$, it then follows that the inflaton field amplitude is expected to evolve as a function of the scale factor $a(t)$ as [59] $\phi \propto a(t)^{-6/(m+2)}$. Thus, in the oscillating regime we have that $V \propto a(t)^{-6m/(m+2)}$, while the inflaton's kinetic energy will behave like $\dot{\phi}^2 \propto a(t)^{-6}$. Thus, for any finite value for the exponent m , with the oscillating phase lasting long enough in the contracting phase, the kinetic energy of the inflaton field will necessarily come to dominate at the bounce. As we are going to show in this section, with the kinetic energy dominating at the bounce, the value of the inflaton field, ϕ_B , will then be uniquely determined at this moment. This result is independent on the details of the contracting phase, provided that the evolution starts sufficiently back in the contracting phase and in the oscillatory regime for the inflaton. The obtained value for ϕ_B for each model provides the initial conditions for the further evolution of the system and which can be carried out up to the end of the accelerated inflationary regime.

In LQC models in which the evolution of the inflaton field is dominated by its kinetic energy at the quantum bounce, a slow-roll inflation phase is practically always reached as demonstrated in many previous papers [10, 29, 30, 33, 34, 36]. Our goal here will be to estimate the number of e -folds of expansion in two regimes: In the preinflationary one, which includes the instant of the bounce until the beginning of slow-roll inflation. We denote this number of e -folds of expansion as N_{pre} . Then, the e -folds from the beginning to the end of inflation, which we call N_{infl} , is also determined. In order to achieve this, let us first begin by analyzing the background dynamics in our scenario starting from the bounce phase. We will proceed without assuming a specific model for the contracting phase.

Immediately before and after the bounce, assumed to happen at a time instant t_B , if the energy density is mostly dominated by kinetic energy as we are going to consider and discussed above, we have a phase of *superdeflation* (for $t < t_B$) and *superinflation* (for $t > t_B$). These are very short phases, which start close to the bounce instant (when $H = 0$, i.e., $\rho = \rho_{\text{cr}}$). They start (at $t < t_B$) and end (at $t > t_B$) when $\dot{H} = 0$. The conditions for superdeflation/superinflation are

$$H^2 \gg |V_{,\phi}|, \quad \dot{\phi}^2/2 \gg V(\phi). \quad (3.1)$$

Right after the superinflation phase, in the postbounce phase, the kinetic energy quickly decreases as $\dot{\phi}^2 \propto 1/a^6$, while the potential energy density $V(\phi)$ only

changes slowly. The inflaton dynamics after the bounce and throughout the preinflationary phase is just monotonic [10]. After a given moment, the potential energy of the inflaton will eventually dominate the energy content of the Universe and the standard slow roll inflationary phase will set in. Before the beginning of slow roll, the quantum corrections to the Friedmann equation are negligible, and the cosmological equations reduce to the usual ones of GR, at which point we then have that

$$\rho_{\text{cr}} \ll \rho, \quad V(\phi) \gg \dot{\phi}^2/2. \quad (3.2)$$

More specifically, the evolution of the Universe for $t \geq t_B$ and prior to reheating (end of inflation) is divided into three different phases: *the bouncing*, *the transition* and *slow-roll inflation* [10]. Next, we describe each of these phases.

A. Kinetic dominated regime

This phase is dominated by the kinetic energy of the inflaton, with $\dot{\phi}^2/2 \gg V(\phi)$. In Eq. (2.5), neglecting the derivative of the potential $V_{,\phi}$, we have

$$\ddot{\phi} + 3H\dot{\phi} \approx 0, \quad (3.3)$$

whose solution is given by

$$\dot{\phi}(t) = \pm \sqrt{2\rho_{\text{cr}}} \left[\frac{a_B}{a(t)} \right]^3, \quad (3.4)$$

where a_B is the scalar factor at the bounce. Substituting the solution (3.4) in Eq. (2.2), we obtain

$$a(t) = a_B \left[1 + \frac{24\pi\rho_{\text{cr}}}{m_{\text{Pl}}^4} \frac{(t - t_B)^2}{t_{\text{Pl}}^2} \right]^{1/6}, \quad (3.5)$$

where $a_B \equiv a(t_B)$ and t_B is the bounce instant. Equation (3.5) gives the expression for the scale factor in the quantum regime of the Universe. In the above equation, $t_{\text{Pl}} = 1/m_{\text{Pl}}$ is the Planck time.

With the analytical solution for $a(t)$, from (3.4) one finds

$$\dot{\phi}(t) = \pm \frac{\sqrt{2\rho_{\text{cr}}}}{\left[1 + \frac{24\pi\rho_{\text{cr}}}{m_{\text{Pl}}^4} (t - t_B)^2/t_{\text{Pl}}^2 \right]^{1/2}}, \quad (3.6)$$

and

$$\phi(t) = \phi_B \pm \frac{m_{\text{Pl}}}{2\sqrt{3}\pi} \operatorname{arcsinh} \left[\sqrt{\frac{24\pi\rho_{\text{cr}}}{m_{\text{Pl}}^4} \frac{(t - t_B)^2}{t_{\text{Pl}}^2}} \right]. \quad (3.7)$$

It is important to notice that even though the result for the inflaton amplitude Eq. (3.7) is derived close to the bounce and where the inflaton potential is negligible, its validity still extends quite well for a long time interval

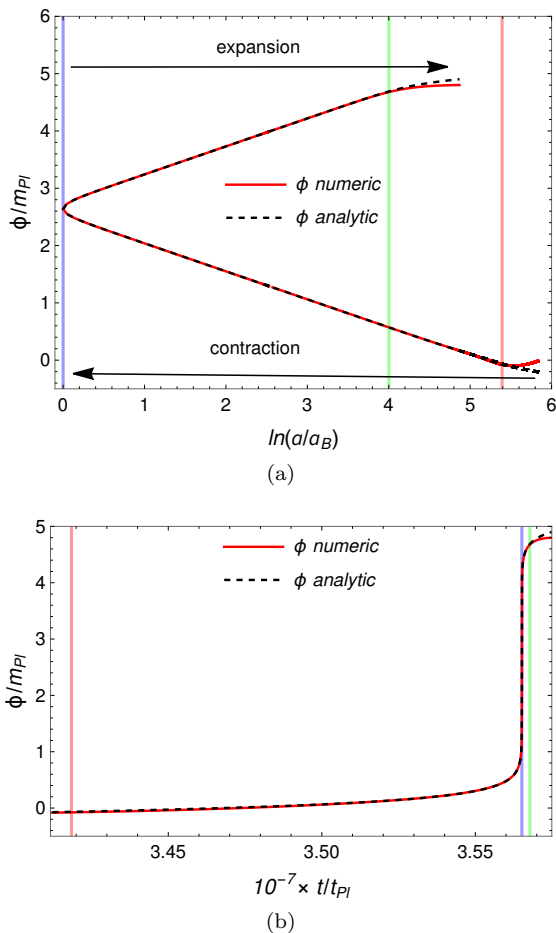


FIG. 1. Comparison of the numerical and analytical results for the inflaton amplitude ϕ . A quadratic power-law potential was considered and initial conditions (set in the contracting phase) such that around 147 e -folds of inflation are generated (see text). The vertical red and green strips indicate the start and end of the kinetic energy dominated regime, $\dot{\phi}^2/2 > V(\phi)$. The vertical blue strip indicates the bounce instant t_B . Evolution is shown in terms of both the number of e -folds [panel (a)] and in terms of the physical time [panel (b)].

both before and after the bounce. This is illustrated in Fig. 1, where we show the numerical evolution for the inflaton amplitude $\phi(t)$ and compare it to the analytical result given by Eq. (3.7). For illustrative purposes, we have considered the quadratic power-law potential, Eq. (2.6), with $n = 1$, but the results remain qualitatively similar when considering other potentials. The initial conditions were considered deep in the contracting phase and such that around 147 e -folds of inflation would be produced. This value of e -folds of inflation was chosen since it is within what is expected for this potential from previous statistical analysis for this form of potential (see, e.g., Refs. [30, 34] for details). The transition time in the contracting and expanding phases, t_{tr}^- and t_{tr}^+ , respectively, defined by $\dot{\phi}^2(t_{tr}^\pm)/2 = V(\phi(t_{tr}^\pm))$, are marked by the red and green vertical strips, respectively. The bounce is

marked by the blue vertical strip. Note that the analytical result for $\phi(t)$ agrees well with the numerical solution obtained when evolving Eq. (2.5) with the Hubble parameter in LQC given by Eq. (2.2) in the whole region $t_{tr}^- \lesssim t \lesssim t_{tr}^+$.

B. Setting the initial conditions

Let us now describe the process of determining the appropriate initial conditions for the evolution of the system and which will determine the inflaton amplitude at the bounce instant, ϕ_B . Having ϕ_B is important because we can straightforwardly relate all relevant postbounce quantities for our analysis with it, as we are going to show below.

First, one notices that for a fluid with equation of state w , we can write the Hubble parameter in LQC as

$$H_{\text{LQC}}(t) = \frac{\frac{4\pi\rho_{\text{cr}}}{m_{\text{Pl}}^4} (1+w) \frac{t-t_B}{t_{\text{Pl}}}}{\left[1 + \frac{6\pi\rho_{\text{cr}}}{m_{\text{Pl}}^4} (1+w)^2 \frac{(t-t_B)^2}{t_{\text{Pl}}^2}\right]} m_{\text{Pl}}, \quad (3.8)$$

which comes straightforwardly when we generalize the scale factor Eq. (3.5) to an arbitrary constant equation of state w . The results derived next hold far from the bounce, where the LQC effects are negligible. Far from the bounce, when the quantum effects can be neglected, *i.e.*, $|t - t_B| \gg t_{\text{Pl}}$, Eq. (3.8) gives the usual expression obtained in GR for a fluid with constant equation of state w ,

$$H \simeq \frac{2}{3(1+w)(t-t_B)}. \quad (3.9)$$

In the following we will assume that the equation of state in Eq. (3.9) can be extended for that of the inflaton field, *i.e.*,

$$w = \frac{\dot{\phi}^2/2 - V(\phi)}{\dot{\phi}^2/2 + V(\phi)}. \quad (3.10)$$

Following also a notation analogous to the one used by the authors of Ref. [33] and defining the ratio of the potential energy to kinetic energy, $\alpha \equiv V/(\dot{\phi}^2/2)$, then the Hubble parameter far from the bounce is approximated as

$$H \simeq \frac{1+\alpha}{3(t-t_B)}, \quad (3.11)$$

where we have used that $w = (1-\alpha)/(1+\alpha)$ in Eq. (3.9). In principle the expression (3.11) might be considered a too rough approximation for the Hubble parameter. But as already noticed before, e.g., from the results shown in Fig. 1, if we look at the dynamics in the contracting phase, for $t_{tr}^- < t < t_B$, it tends to be much slower than in the expanding phase, for $t_B < t < t_{tr}^+$, which gives us hope that we can eventually match the results at some point in the contracting phase with some value

of α and then evolve the system forward to the bounce instant. As suggested from the results shown in Fig. 1 and the above discussion, the appropriate moment to perform such matching is well before the bounce, while in the contracting phase, but where the quantum effects are still negligible and we can use Eq. (3.11), but after the transition time t_{tr}^- , where we can still apply Eqs. (3.6) and (3.7) with good accuracy. Our results to be shown in Sec. IV indeed indicate that this simple strategy is a sound one.

Our approximation then consists of considering the dynamics at some point in the contracting phase, after the transition time t_{tr}^- , but still well before the bounce, such that the quantum effects are still negligible. We then look at some instant t_α in the contracting phase given by $t_{tr}^- < t_\alpha \ll t_B$, and where the Hubble parameter can be approximated by Eq. (3.11). Taking the time derivative of Eq. (3.11) and equating it to $-4\pi\dot{\phi}^2/m_{\text{Pl}}^2$, which is valid in the regime we are considering (*i.e.*, far from the bounce and where the quantum effects are still negligible), we find a direct relation between the potential and its field derivative, V' , as given by

$$\frac{V(\phi_\alpha)}{V'(\phi_\alpha)} = \frac{\sqrt{1+\alpha}}{4\sqrt{3\pi}} m_{\text{Pl}}. \quad (3.12)$$

To obtain Eq. (3.12), we have used the inflaton's equation of motion Eq. (2.5) along also with Eq. (3.11) to eliminate the explicit time dependence in favor of the Hubble parameter and finally that²

$$H = -\sqrt{\frac{8\pi}{3m_{\text{Pl}}^2} \frac{(1+\alpha)}{\alpha}} V, \quad (3.13)$$

which follows when using that $\dot{\phi}^2/2 \equiv V/\alpha$. Our approximation to estimate ϕ_B now consists of considering that we can take an ‘‘average’’ value for α and approximate it as a constant $\bar{\alpha}$. In this case, for a given value of $\bar{\alpha}$ within the range $(0, 1)$ we can readily estimate the inflaton amplitude $\phi_\alpha \equiv \phi(t_\alpha)$, for any given potential, when using Eq. (3.12), and also the instant of time t_α when using Eqs. (3.11) and (3.13) for $\alpha \rightarrow \bar{\alpha}$,

$$t_\alpha - t_B = -\frac{1+\bar{\alpha}}{3} \sqrt{\frac{3m_{\text{Pl}}^2 \bar{\alpha}}{8\pi(1+\bar{\alpha})V(\phi_\alpha)}}. \quad (3.14)$$

Here we fix the value for $\bar{\alpha}$ such that the dynamics will match the one obtained for each potential and which results are available for the potentials we are analyzing. We note that this strategy is analogous to the one adopted, *e.g.*, by the authors of Ref. [33], where the constant value for $\bar{\alpha}$ was fixed by matching their numerical results for

ϕ , but in the postbounce regime instead. The apparent arbitrariness in having to choose a different value of $\bar{\alpha}$ for different initial conditions has also been dealt with in Ref. [33] by fixing $\bar{\alpha}$ for one initial condition and then using the *same* value for all other cases. Thus, there is only one value of $\bar{\alpha}$ fixed once and for all. As shown in Ref. [33], this simple approach was good enough to reproduce their numerical results in the postbounce phase when considering different initial conditions taken at the bounce instant. Here we avoid applying this to the postbounce regime and choose to consider its application in the contracting phase instead. This is justified because, as seen from Fig. 1(b), the postbounce dynamics lasting from the bounce up to the transition time t_{tr}^+ is much shorter than the one lasting from t_{tr}^- in the contracting phase until the bounce time t_B . The ratio of energies α changes much faster in the expanding phase than in the contracting one. Trying to fix α to match the numerical results in the expanding phase and evolving back to the bounce instant t_B to obtain ϕ_B for example, thus implies requiring a much higher accuracy than the one we can achieve doing the same procedure in the contracting phase. Motivated also by the results obtained by the authors of Ref. [33], we will fix the value of $\bar{\alpha}$ such that our analytical results will match the statistical analysis considered for example in Ref. [30]. Furthermore, we also show that we only need to fix the value of $\bar{\alpha}$ once for one primordial inflaton potential. This same value can then be used for all other potentials. We will see that this simple strategy will produce results with good accuracy as confirmed by the results shown in Sec. IV.

C. The postbounce transition time and the inflaton amplitude

Having both ϕ_α and the instant t_α for a given value of $\bar{\alpha}$ by following the above procedure in the contracting phase, we then can use Eq. (3.7) to obtain the inflaton amplitude at the bounce time, ϕ_B . Given the value for ϕ_B , we can estimate the number of *e*-folds of inflation. First, the inflaton value at the transition time t_{tr}^+ in the postbounce regime is determined by using Eq. (3.7) again,

$$\phi(t_{tr}^+) = \phi_B + \frac{m_{\text{Pl}}}{2\sqrt{3\pi}} \operatorname{arcsinh} \left(\sqrt{\frac{24\pi\rho_{\text{cr}}}{m_{\text{Pl}}^4} \frac{t_{tr}^+ - t_B}{t_{\text{Pl}}}} \right). \quad (3.15)$$

We can now consider that at the transition time we have that³

$$\dot{\phi}(t_{tr}^+) = \sqrt{2V(\phi(t_{tr}^+))}. \quad (3.16)$$

² Note the choice of minus sign for the Hubble parameter is because we are considering the dynamics in the contracting phase, hence, $H < 0$.

³ Note that we could have this equation for both signs positive or negative for $\dot{\phi}$. Throughout this paper, we work with the convention of adopting the positive sign for $\dot{\phi}$, thus also considering the positive sign in Eq. (3.7) when writing it for $t = t_{tr}^+$ in Eq. (3.15). This implies that the field is always moving from

By using the time derivative of $\phi(t)$, Eq. (3.6) at t_{tr}^+ and substituting Eq. (3.15) in Eq. (3.16), we can then numerically⁴ solve Eq. (3.16) for the time interval $t_{tr}^+ - t_B$. This result then also allows us to obtain $\phi(t_{tr}^+)$ when substituting the solution for $t_{tr}^+ - t_B$ back in Eq. (3.15).

D. Beginning of the slow-roll inflationary phase

When the slow-roll phase starts at some time $t_i > t_{tr}^+$, the Universe is already far from the quantum regime. The potential energy starts to dominate over the kinetic energy giving rise to the inflationary regime. In the following, we use the index ‘‘i’’ to denote the quantities at the beginning of inflation, which corresponds to the moment when the Universe starts accelerating and the equation of state satisfies $w \leq -1/3$. In order to obtain the quantities in this moment, we can use the expansion for $\phi(t)$ which is valid for $t \simeq t_i$,

$$\phi_i \simeq \phi_{tr} + \dot{\phi}_{tr} t_{tr}^+ \ln \frac{t_i}{t_{tr}^+}, \quad (3.17)$$

where $\phi_{tr} \equiv \phi(t_{tr}^+)$, $\dot{\phi}_{tr} \equiv \dot{\phi}(t_{tr}^+)$ and, without loss of generality, we are setting from this point on that $t_B = 0$. Likewise for $\dot{\phi}(t_i)$, we have that

$$\dot{\phi}_i \simeq \frac{t_{tr}^+}{t_i} \dot{\phi}_{tr}. \quad (3.18)$$

Thus,

$$V(\phi_i) \simeq V(\phi_{tr}) + V_{,\phi}(\phi_{tr}) t_{tr}^+ \dot{\phi}_{tr} \ln \frac{t_i}{t_{tr}^+}. \quad (3.19)$$

Since the accelerated regime, $\ddot{a} > 0$, starts at $w = -1/3$ for the equation of state, then

$$\dot{\phi}_i^2 = V(\phi_i). \quad (3.20)$$

Using Eqs. (3.20) and (3.19) and knowing t_{tr}^+ and ϕ_{tr} obtained from the previous step, we can now numerically

the left to the right side of the potential. For the power law and Higgs potentials this choice does not lead to any ambiguity since the potential is symmetric and for any choice of the sign for $\dot{\phi}$ the field is always climbing the potential when starting the initial conditions deep inside the contracting phase and always close to the minimum of the potential. The Starobinsky potential is asymmetric, but for the standard form, Eq. (2.8), inflation only happens along the flat region, which resides in the right-hand side of the potential.

⁴ In fact exact analytical expressions for both $t_{tr}^+ - t_B$ and $\phi(t_{tr}^+)$ can be obtained from these equations by approximating them by considering that $t_{tr}^+ - t_B \gg t_{Pl}$ (see, e.g., Ref. [10] for details in the cases of the quadratic power law and Starobinsky potentials). The solution is in general expressed in terms of Lambert functions. Here we simply choose to directly numerically solve Eq. (3.16), which can in principle be done for any potential in general.

solve⁵ Eq. (3.20) for the initial time t_i , which will then determine ϕ_i from Eq. (3.17).

E. Number of e -folds N_{pre} and N_{infl}

The number of e -folds of expansion is defined as

$$N \equiv \ln \left(\frac{a_{end}}{a_{init}} \right), \quad (3.21)$$

where a_{init} and a_{end} denote, respectively, the scale factors at the beginning and at the end of the corresponding period.

Let us first present the results for the preinflationary phase, i.e., the expansion lasting from the bounce time to the start of the inflationary phase. The number of e -folds for the preinflationary phase is denoted by N_{pre} , with $N_{pre} \equiv \ln(a_i/a_B)$, where a_B and a_i are the scale factors at the bounce and at the beginning of inflation, respectively. According to what we have done in the previous sections, we can write a_i as [10]

$$a_i \simeq a_{tr} \left(1 + t_{tr}^+ H_{tr} \ln \frac{t_i}{t_{tr}^+} \right), \quad (3.22)$$

where H_{tr} in Eq. (3.22) is obtained from the Friedmann equation considering $\rho_{tr} = \dot{\phi}_{tr}^2/2 + V(\phi_{tr})$. Therefore, the number of e -folds of expansion in the preinflationary phase can be written as

$$\begin{aligned} N_{pre} &= \ln \left(\frac{a_i}{a_B} \right) = \ln \left(\frac{a_{tr}}{a_B} \right) + \ln \left(\frac{a_i}{a_{tr}} \right) \\ &\simeq \frac{1}{6} \ln \left(1 + \frac{24\pi\rho_{cr}}{m_{Pl}^4} \frac{(t_{tr}^+)^2}{t_{Pl}^2} \right) + \ln \left(1 + t_{tr}^+ H_{tr} \ln \frac{t_i}{t_{tr}^+} \right), \end{aligned} \quad (3.23)$$

where we have used Eq. (3.5) at $t = t_{tr}^+$ and Eq. (3.22).

The number of the e -folds of expansion during the inflationary phase, N_{infl} , is defined as,

$$N_{infl}(\phi) \equiv \ln \left(\frac{a_{end}}{a_i} \right) \approx \frac{8\pi}{m_{Pl}^2} \int_{\phi_{end}}^{\phi_i} \left(\frac{V}{\dot{V}} \right) d\phi, \quad (3.24)$$

where in the last term in the above equation we have used the slow-roll approximations, valid during inflation, $\dot{\phi} \simeq -V_{,\phi}/(3H)$ and $H^2 \simeq 8\pi V/(3m_{Pl}^2)$. The total number of e -folds lasting from the bounce until the end of inflation is then $N_{total} = N_{pre} + N_{infl}$. In Eq. (3.24), ϕ_i is given by Eq. (3.17) and ϕ_{end} , the scalar field at the end of the inflationary phase, is obtained by the slow-roll coefficient $\epsilon = -\dot{H}/H^2$ when it is set to one (indicating the end of the accelerated regime). Thus, from $\epsilon = -\dot{H}/H^2 \simeq (V_{,\phi} m_{Pl}/V)^2/(16\pi) = 1$, ϕ_{end} can be readily obtained for each of the potential forms we are considering. The results are explicitly given below.

⁵ Again, it can be found general analytical solutions for Eq. (3.20) which are expressed also in terms of Lambert functions [10], but for practical purposes we just opt to numerically solve Eq. (3.20).

1. The power-law monomial potentials

From Eq. (3.24), N_{infl} in the case of monomial potentials is given by

$$N_{\text{infl}} = \frac{2\pi}{n m_{\text{Pl}}^2} (\phi_i^2 - \phi_{\text{end}}^2), \quad (3.25)$$

with ϕ_{end} given by

$$\phi_{\text{end}}^2 = \frac{n^2}{4\pi} m_{\text{Pl}}^2. \quad (3.26)$$

2. The Higgs-like symmetry breaking potential

For the Higgs-like potential we have that

$$N_{\text{infl}} = \frac{2\pi}{m_{\text{Pl}}^2} \left[\frac{\phi_i^2 - \phi_{\text{end}}^2}{2} - v^2 \ln \frac{\phi_i}{\phi_{\text{end}}} \right] \quad (3.27)$$

and

$$\phi_{\text{end}} = \pm \sqrt{v^2 + \frac{m_{\text{Pl}}^2}{2\pi}} \pm \frac{m_{\text{Pl}}^2}{2\pi} \sqrt{1 + \frac{4\pi v^2}{m_{\text{Pl}}^2}}, \quad (3.28)$$

where the signs positive and negative correspond to the large and small-field cases, respectively.

3. The Starobinsky potential

For the Starobinsky potential we obtain that

$$N_{\text{infl}} = \frac{3}{4} \left(e^{\sqrt{\frac{16\pi}{3}} \frac{\phi_i}{m_{\text{Pl}}}} - e^{\sqrt{\frac{16\pi}{3}} \frac{\phi_{\text{end}}}{m_{\text{Pl}}}} \right) + \frac{\sqrt{3\pi}}{m_{\text{Pl}}} (\phi_i - \phi_{\text{end}}), \quad (3.29)$$

where

$$\phi_{\text{end}} = m_{\text{Pl}} \sqrt{\frac{3}{16\pi}} \ln \left(1 + \frac{2}{\sqrt{3}} \right). \quad (3.30)$$

Having derived and collected all relevant equations, we are now in condition to present our results in the following section.

IV. RESULTS

As explained in Sec. III B, we first need to set an appropriate value for the ratio $\bar{\alpha}$ of potential to kinetic energy in the contracting phase. We illustrate this by comparing the results generated for the number of e -folds, Eq. (3.24), within our approach to those obtained through the statistical analysis produced in Ref. [30]. In Ref. [30], which follows the proposal initiated by the authors of Ref. [34], initial conditions are generated deep inside the contracting phase, where $\rho_\phi \ll \rho_{\text{cr}}$, and the

inflaton is oscillating around the minimum of its potential. The number of e -folds of inflation is then obtained by taking a large number of random initial conditions satisfying these conditions and each one of them is evolved up to the end of inflation. The probability distribution function for each potential is obtained, from which statistical predictions for the number of e -folds are derived. In Ref. [30] results were obtained for the power-law potential with $n = 1, 2, 3$ and also for the Higgs-like potential for different values for the VEV v . These results of Ref. [30] are indicated, for comparison, by the data points with the error bars shown in Fig. 2, for the case of the power-law potential, and in Fig. 3, for the case of the Higgs-like potential.

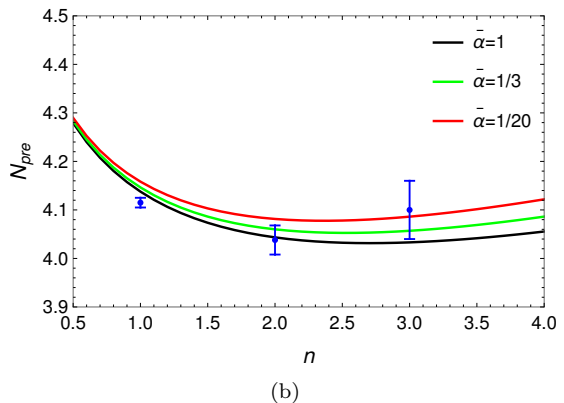
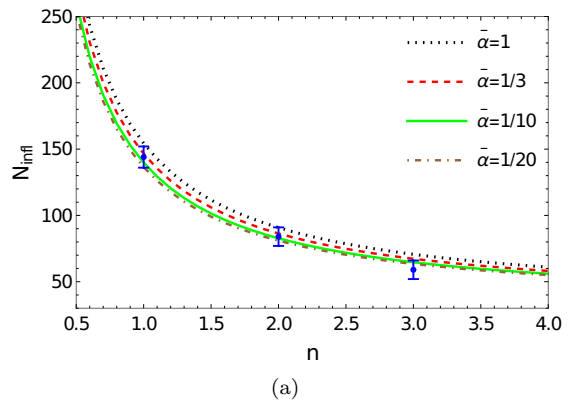


FIG. 2. The numerical results for the number of e -folds of inflation [panel (a)] and for the number of e -folds for the pre-inflationary regime lasting from the bounce until the beginning of inflation [panel (b)] obtained through the method described in Sec. III E when applied to the monomial power-law potential Eq. (2.6). The data points show the results obtained in Ref. [30].

From the results shown in Fig. 2, we see that the results very reasonably fit the data points, with a difference of less than 5%, for the choice⁶ $\bar{\alpha} = 1/3$. The same

⁶ We note that the same value for the constant α given by 1/3

choice of $\bar{\alpha}$ is also seen to reproduce well the results for the Higgs-like potential, for many different values for v , as shown in Fig. 3. Note that for the Higgs-like potential curves do not quite agree with the data points for the preinflationary number of e -folds, but the qualitative agreement is still very good, again within less than 5% differences.⁷ Hence, our results indicate that we can just fix $\bar{\alpha} = 1/3$ once and for all other primordial potentials it should also continue to produce sufficiently accurate results. This is what we have assumed in all our subsequent results shown next.

As already said above, the results shown in Figs. 2 and 3, all our subsequent analysis will be done by choosing $\bar{\alpha} = 1/3$. Recalling that α is related to the equation of state by $w = (1 - \alpha)/(1 + \alpha)$, hence, the choice $\bar{\alpha} = 1/3$ is also equivalent to considering the moment t_α in the contracting phase where $w = 1/2$.

Figures 2 and 3 already show some revealing features. One recalls that one typically requires at least around 80 e -folds of total expansion from the bounce to the end of inflation in order for the quantum effects on the spectra to be sufficiently diluted [10]. On the contrary, if the total expansion lasts less than this minimum, the LQC effects on the spectra would already be visible. This limitation, which is a consequence of the effects of LQC on the power spectrum, will be detailed below in the next section. From Fig. 2(a), therefore, it indicates that monomial power-law potentials with a fifth power in the inflaton ($n = 2.5$) and higher are not favored due to the small amount of expansion predicted from them. For the quadratic potential ($n = 1$) the situation is quite different. We obtain $N_{\text{infl}} \sim 147$, in agreement with previous results obtained in Ref. [34]. Despite being in agreement with current CMB data, such high value for N_{infl} does not lead to good prospects in observing signals from the high energy regime on CMB data. On the other hand, for the quartic model ($n = 2$) we obtain $N_{\text{infl}} \sim 87$. This value, while providing a satisfactory number of e -folds of inflation, it also allows for better prospects concerning potentially observable signals from the quantum regime of LQC on future CMB measurements. In Fig. 3(a), which shows our results for the Higgs-like potential when inflation happens in the large-field portion of the potential, i.e., $|\phi| > |v|$, the number of e -folds is always larger than $N_{\text{infl}} \sim 87$, whose value is approached when $v \rightarrow 0$ and the model is analogous to the quartic monomial potential. However, when inflation happens in the plateau region of the potential, i.e., when $|\phi| < |v|$, the number

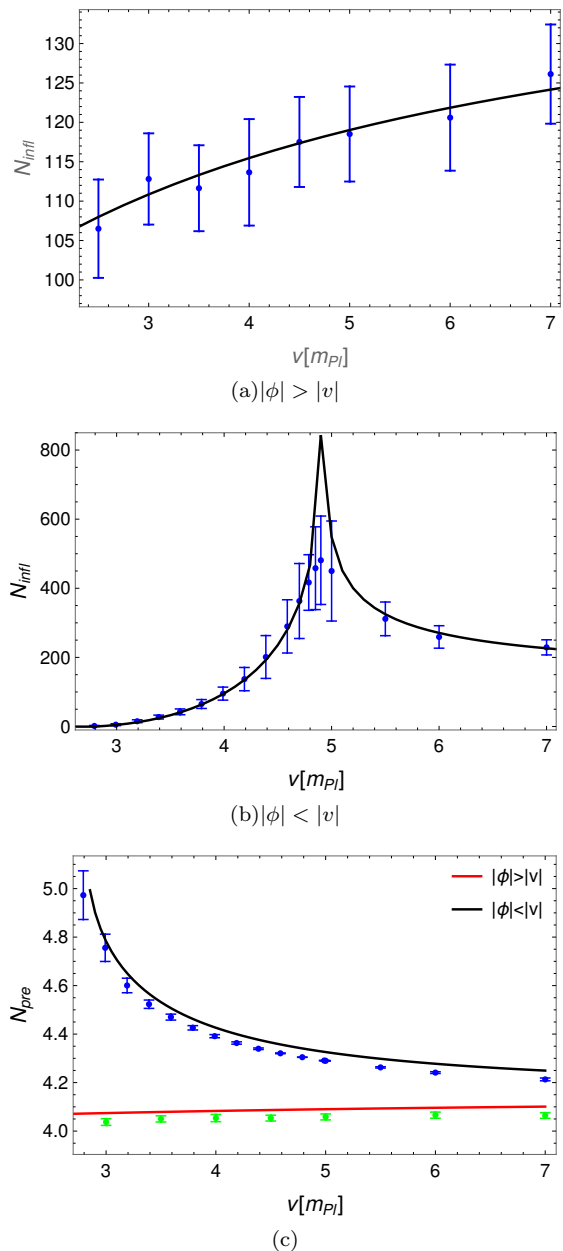


FIG. 3. The numerical results for the number of e -folds of inflation in the case of the Higgs-like potential when inflation happens in the large-field portion of the potential, $|\phi| > |v|$ [panel (a)], and for inflation happening around the plateau region, $|\phi| < |v|$ [panel (b)]. The number of e -folds for the preinflationary regime lasting from the bounce until the beginning of inflation is shown in panel (c). The data points are the results obtained using the methods described in Ref. [30]. All curves here were obtained by setting $\bar{\alpha} = 1/3$ within the procedure described in Sec. III B.

was, coincidentally, also found by the authors of Ref. [33], though matching their numerical results that were obtained in the post-bounce phase.

⁷ We notice that for all data points shown in the figures, the error bars are the one-standard deviation from the average values.

of e -folds tends initially to increase with the value of the VEV v , up to around $v \sim 5m_{\text{Pl}}$, after which it drops and tends to asymptote around $N_{\text{infl}} \sim 200$. This behavior was already hinted in the analysis done in Ref. [30] but it becomes clear now in the results shown in Fig. 3(b).

This apparently odd behavior has a simple explanation. For small VEV values, the plateau region of the potential is small and it is difficult to localize the inflaton in that small field region of the potential and the number of e -folds of inflation tends to be small. As the VEV increases, it becomes more likely for inflation to happen closer to the flatter top of the potential and the number of e -folds of inflation increases⁸. However, for even larger values for the VEV, it becomes again less likely that the dynamics would put the inflaton too close to the top of the potential and the number of e -folds decreases. Our results indicate that there is an optimum value for the VEV for inflation having a maximum number of e -folds for a Higgs-like potential in the context of LQC and this value for the VEV is around $v \sim 5m_{\text{Pl}}$. On the other hand, our results also show that for $v \lesssim 3m_{\text{Pl}}$, there are essentially no more initial conditions leading to inflation starting and ending in the plateau region, which also agrees with the findings of Ref. [60].

Our results, including also the ones for the Starobinsky potential, Eq. (2.8), are summarized in Tables I-IV. We have chosen the cases of a quadratic, a quartic and a sextic monomial potential for illustration, along with some representative cases of the Higgs-like potential and then the Starobinsky potential.

In Tables I and II we give the results for the various quantities which were defined in the previous section, in particular the numerical prediction for the amplitude for the inflaton field at the bounce, ϕ_{B} . This is important, since all other quantities, in particular the point where inflation starts, depends on this value. In a sense, we see that this is equivalent to providing the initial conditions at the bounce time. The subsequent evolution of the Universe is then completely determined from these initial conditions, especially the inflationary regime. In this case, knowing the initial conditions at the bounce, we have shown that it completely determines the duration of inflation for any given potential. Note that the predicted total duration of inflation here is based on assuming a kinetic-dominated bounce and using $\alpha = 1/3$, differently from the statistical results obtained for example in Refs. [30, 34–37]. The predicted values for the duration of the preinflationary phase and inflation are shown in Tables III and IV.

From the results shown in Tables III and IV, we can see that for all models studied the number of preinflationary e -folds, which consider the expansion from the bounce to the beginning of the slow-roll inflation, is always $N_{\text{pre}} \sim 4 - 5$, which agrees with Ref. [30] and other

previous references. This is a consequence of the bounce being dominated by the kinetic energy of the inflaton field, thus, being weakly dependent on the form of its potential. For the number of inflationary e -folds, we also obtain results generically in agreement with those obtained in Ref. [30]. In particular, we can observe that for the Starobinsky potential $N_{\text{infl}} \sim 10^9$, i.e., the duration of slow-roll inflation is longer compared to the other models. This is consistent with the results shown, e.g., in Ref. [37], which follows the determination for the number of e -folds of inflation originally proposed in Ref. [34] and which was also considered in Ref. [30]. This happens for positive values of the scalar field at the beginning of inflation, i.e., where the potentials have a plateau [61]. As discussed in Ref. [37], LQC dynamics automatically provides highly energetic field configurations at the onset of inflation. Consequently, in these cases the inflaton field is “pushed” away on the plateau, leading to a very long phase of slow-roll inflation. It is important to remember that potentials predicting a large number of e -folds are perfectly fine as far as the observations are concerned. For the monomial power-law potentials, as already seen in a previous work [30], increasing the power n implies a decreasing of the number of e -folds.

V. CONSTRAINING THE BARBERO-IMMIRZI PARAMETER

As previously discussed, the Barbero-Immirzi parameter is strictly a free parameter of the theory. Therefore, it is important to find ways to constraint its value. In this section we study how the prediction for the number of e -folds in LQC helps in setting possible constraints on the Barbero-Immirzi parameter γ .

In order to constrain this parameter, we will need to analyze the power spectrum in LQC, as we explain in the following. In order to treat the perturbations in LQC we are going to adopt the so-called dressed metric quantization approach [62]. The dressed metric approach, in addition of being one of the approaches most studied in the literature, is the approach that seems most suitable for this kind of analysis. It reproduces qualitatively similar results for the power spectrum as the hybrid quantization approach [63]. In general, both the quantization scheme and the initial conditions chosen are important when deriving the power spectrum in LQC. Concerning the initial conditions, the most commonly used is the BD vacuum state imposed in the contracting phase, prior to the bounce. Since before the start of the bouncing phase all the important modes are within the effective horizon, the BD vacuum state is a natural choice in this case. A second possibility would be to impose initial conditions at the bounce. At the bounce some modes are inside the effective horizon and some are outside it. So, in this case the BD vacuum state is no longer a suitable choice. Instead, one can impose the fourth-order adiabatic vacuum state [62]. Within the validity of the latter, it has been

⁸ It should be noticed that the number of e -folds in Fig. 3(b) appears to grow very sharp at around $v \simeq 5m_{\text{Pl}}$, we expect the real situation to display a smoother maximum as actually indicated by the numerical data. This is because there is always Gaussian stochastic quantum fluctuations acting on the background inflaton field [60]. These fluctuations make unlikely for the inflaton to be precisely localized at the top of the maximum of the potential at $\phi = 0$.

TABLE I. Numerical values obtained for the three forms of monomial potentials and the Starobinsky potential.

Model	V_0/m_{Pl}^4	$\phi_{\text{B}}/m_{\text{Pl}}$	$t_{\text{tr}}^+/t_{\text{Pl}}$	$\phi_{\text{tr}}/m_{\text{Pl}}$	$(10^6)\dot{\phi}_{\text{tr}}/m_{\text{Pl}}^2$	t_i/t_{Pl}	ϕ_i/m_{Pl}
Quadratic	1.355×10^{-12}	2.72	2.9×10^4	4.72	5.6	4.1×10^4	4.84
Quartic	1.373×10^{-13}	3.19	2.3×10^4	5.22	7.1	3.2×10^4	5.27
Sextic	4.563×10^{-15}	3.65	2.3×10^4	5.68	7.1	3.1×10^4	5.73
Starobinsky	1.497×10^{-13}	2.65	3.0×10^5	5.10	0.5	4.2×10^5	5.16

TABLE II. Numerical values obtained for the Higgs-like potential, considering some illustrative values for the VEV.

Model	V_0/m_{Pl}^4	$\phi_{\text{B}}/m_{\text{Pl}}$	$t_{\text{tr}}^+/t_{\text{Pl}}$	$\phi_{\text{tr}}/m_{\text{Pl}}$	$(10^6)\dot{\phi}_{\text{tr}}/m_{\text{Pl}}^2$	t_i/t_{Pl}	ϕ_i/m_{Pl}
Higgs-like ($ \phi_{\text{B}} > v = 3.5m_{\text{Pl}} $)	2.867×10^{-14}	6.27	2.4×10^4	8.30	6.8	3.3×10^4	8.35
Higgs-like ($ \phi_{\text{B}} > v = 4.0m_{\text{Pl}} $)	2.384×10^{-14}	6.76	2.4×10^4	8.80	6.7	3.4×10^4	8.85
Higgs-like ($ \phi_{\text{B}} > v = 4.5m_{\text{Pl}} $)	2.010×10^{-14}	7.25	2.5×10^4	9.29	6.6	3.4×10^4	9.35
Higgs-like ($ \phi_{\text{B}} < v = 3.5m_{\text{Pl}} $)	6.424×10^{-14}	-0.79	9.0×10^4	1.46	1.8	1.3×10^5	1.52
Higgs-like ($ \phi_{\text{B}} < v = 4.0m_{\text{Pl}} $)	5.245×10^{-14}	-1.30	6.6×10^4	0.90	2.5	9.4×10^4	0.96
Higgs-like ($ \phi_{\text{B}} < v = 4.5m_{\text{Pl}} $)	4.254×10^{-14}	-1.80	5.6×10^4	0.37	2.9	7.9×10^4	0.43

TABLE III. Number of e -folds obtained through the analytical analysis for the same models considered in Table I.

Model	N_{pre}	N_{infl}
Quadratic	4.15	146.55
Quartic	4.06	86.36
Sextic	4.06	67.30
Starobinsky	4.92	1.10×10^9

TABLE IV. Number of e -folds obtained for the Higgs-like potential, assuming different values for the VEV.

Model	N_{pre}	N_{infl}
Higgs-like ($ \phi_{\text{B}} > v = 3.5m_{\text{Pl}} $)	4.08	113.31
Higgs-like ($ \phi_{\text{B}} > v = 4.0m_{\text{Pl}} $)	4.08	115.46
Higgs-like ($ \phi_{\text{B}} > v = 4.5m_{\text{Pl}} $)	4.09	117.35
Higgs-like ($ \phi_{\text{B}} < v = 3.5m_{\text{Pl}} $)	4.53	32.64
Higgs-like ($ \phi_{\text{B}} < v = 4.0m_{\text{Pl}} $)	4.43	95.66
Higgs-like ($ \phi_{\text{B}} < v = 4.5m_{\text{Pl}} $)	4.37	235.92

shown in the literature [10] that both choices essentially lead to the same results.

A. The power spectrum in LQC

The quantum bounce changes the scalar power spectrum by a correction term which depends on the characteristic scale at the bounce. This characteristic scale is the shortest scale (or largest wave number, namely k_{B}) that feels the spacetime curvature during the bounce. In previous works (see, for instance, Ref. [53]), precise constraints on the correction term in the scalar power spectrum of LQC was obtained using the recent CMB data, providing limits on the characteristic scale k_{B} . It happens that this scale is a function of the Barbero-Immirzi parameter and the number of e -folds of expansion from the bounce until today, N_{T} . Therefore, in the following we use such observational constraints on k_{B} in order to impose limits on the value of γ as a function of the e -fold number.

In addition to the modifications at the background level from LQC, at the perturbative level modifications are also expected, especially from relevant modes which have physical wavelengths comparable to the curvature radius at the bounce time. Unlike what happens in GR, where it is usually assumed that the preinflationary dynamics does not have any effect on modes observable in the CMB, in LQC the situation is different. Modes that experience curvature are excited in the Planck regime around the bounce time. The main effect at the onset of inflation is that the quantum state of perturbations is populated by excitations of these modes over the BD vacuum. As a consequence, the scalar curvature power spectrum in LQC gets modified with respect to GR, such

that it can be written as (see Ref. [10] for more details)

$$\begin{aligned}\Delta_{\mathcal{R}}(k) &= |\alpha_k + \beta_k|^2 \Delta_{\mathcal{R}}^{GR}(k) \\ &= (1 + 2|\beta_k|^2 + 2\text{Re}(\alpha_k \beta_k^*)) \Delta_{\mathcal{R}}^{GR}(k).\end{aligned}\quad (5.1)$$

In Eq. (5.1) α_k and β_k are the Bogoliubov coefficients, where the preinflationary effects are codified, and $\Delta_{\mathcal{R}}^{GR}$ is the GR form for the power spectrum. In GR with the BD vacuum, the Bogoliubov coefficients in Eq. (5.1) should reduce simply to $\alpha_k \rightarrow \alpha_k^{\text{BD}} = 1$, and $\beta_k \rightarrow \beta_k^{\text{BD}} = 0$. In LQC, the change of the spectrum can be seen exactly as a result of the change of the vacuum state with respect to the GR case, since $|\beta_k|^2 \equiv n_k$ is associated with the number of excitations in the mode k .

Equation (5.1) can also be parametrized as

$$\Delta_{\mathcal{R}}(k) = (1 + \delta_{PL}) \Delta_{\mathcal{R}}^{GR}(k), \quad (5.2)$$

where the factor δ_{PL} is a scale (k -)dependent correction, which, following the derivation given in Ref. [10], is given by

$$\begin{aligned}\delta_{PL} &= \left[1 + \cos\left(\frac{\pi}{\sqrt{3}}\right) \right] \text{csch}^2\left(\frac{\pi k}{\sqrt{6}k_B}\right) \\ &+ \sqrt{2} \sqrt{\cosh\left(\frac{2\pi k}{\sqrt{6}k_B}\right) + \cos\left(\frac{\pi}{\sqrt{3}}\right)} \cos\left(\frac{\pi}{2\sqrt{3}}\right) \\ &\times \text{csch}^2\left(\frac{\pi k}{\sqrt{6}k_B}\right) \cos(2k\eta_B + \varphi_k),\end{aligned}\quad (5.3)$$

where

$$\varphi_k \equiv \arctan \left\{ \frac{\text{Im}[\Gamma(a_1)\Gamma(a_2)\Gamma^2(a_3 - a_1 - a_2)]}{\text{Re}[\Gamma(a_1)\Gamma(a_2)\Gamma^2(a_3 - a_1 - a_2)]} \right\}, \quad (5.4)$$

with a_1, a_2, a_3 defined as $a_{1,2} = (1 \pm 1/\sqrt{3})/2 - ik/(\sqrt{6}k_B)$ and $a_3 = 1 - ik/(\sqrt{6}k_B)$. In particular, η_B is the conformal time at the bounce and $k_B = \sqrt{\rho_c} a_B \sqrt{8\pi}/m_{\text{Pl}}$ is the characteristic scale also at the bounce.

From the above equations, we identify

$$2|\beta_k|^2 = \left[1 + \cos\left(\frac{\pi}{\sqrt{3}}\right) \right] \text{csch}^2\left(\frac{\pi k}{\sqrt{6}k_B}\right), \quad (5.5)$$

$$\begin{aligned}2\text{Re}(\alpha_k \beta_k^*) &= \sqrt{2} \sqrt{\cosh\left(\frac{2\pi k}{\sqrt{6}k_B}\right) + \cos\left(\frac{\pi}{\sqrt{3}}\right)} \\ &\times \cos\left(\frac{\pi}{2\sqrt{3}}\right) \text{csch}^2\left(\frac{\pi k}{\sqrt{6}k_B}\right) \cos(2k\eta_B + \varphi_k).\end{aligned}\quad (5.6)$$

The term $\cos(2k\eta_B + \varphi_k)$ in Eq. (5.6) oscillates very fast, having a negligible effect when averaging out in time. Therefore, for practical purposes, in observable quantities the factor δ_{PL} can be simply considered as being given by

$$\delta_{PL} = \left[1 + \cos\left(\frac{\pi}{\sqrt{3}}\right) \right] \text{csch}^2\left(\frac{\pi k}{\sqrt{6}k_B}\right). \quad (5.7)$$

Note that in this case δ_{PL} can simply be identified with $2n_k$, i.e., with the number of excitations in the mode k which appears as a consequence of the quantum bounce in LQC. It is due to this correction term that in LQC, in order for the spectrum to be consistent with the observations, it is required that the Universe must have expanded some extra 21 e -folds such as to allow for those scale-dependent features in the primordial scalar power spectrum to get sufficiently diluted and as discussed in detail in Refs. [10, 53].

Even though the correction given by Eq. (5.7) was derived in the dressed metric quantization approach, the result is also qualitatively similar when derived in the hybrid quantization approach (see, e.g., Ref. [64]). Other alternative quantization schemes used in LQC can lead to corrections to the power spectrum that are suppressed. This seems to be the case, for example, in the closed/deformed algebra approach [65, 66]. In this case there is no need in principle of the additional extra e -folds of expansion as required in the dressed or hybrid quantization approaches. Either way, we can view our results using the dressed metric approach as the one giving the most restrictive condition on the required minimum number of e -folds. Even in other approaches that might lead to a suppressed correction to the power spectrum, one still needs to require that inflation lasts around some 60 or so e -folds. This still gives a restriction qualitatively similar to what we will consider below, though weaker.

B. The Barbero-Immirzi parameter as a function of the number of e -folds

The total number of e -folds of expansion from the moment of the bounce until today, N_{T} , is related to the LQC parameter k_B . By assuming an upper bound on k_B , it can be translated into constraints on the total number of e -folds. We are interested in finding an upper bound value for k_B , which implies in a lower value for the number of e -folds. In Ref. [53], for example, constraints on the parameter k_B were obtained from CMB data. Since k_B is related to γ , these results can be translated into constraints in the parameter γ .

The relation between k_B and the number of e -folds is given by the equation

$$k_B \equiv \frac{\sqrt{8\pi\rho_{\text{cr}}} a_B}{m_{\text{Pl}}} = m_{\text{Pl}} \left(\frac{\sqrt{3}}{4\pi\gamma^3} \right)^{1/2} e^{-N_{\text{T}}}, \quad (5.8)$$

where we have used Eq. (2.3) and in the above equation $N_{\text{T}} = \ln(a_0/a_B)$ is the total number of e -folds from the bounce until today. Note that in Eq. (5.8) we have used the standard convention of setting the scale factor today as one, $a_0 = 1$.

It happens that the CMB observations constrain directly the value of k_B by imposing a limit in the correction term given by Eq. (5.7). An updated observation constraint on k_B was obtained in Ref. [53], which leads to

$k_B < 1.9 \times 10^{-4} \text{ Mpc}^{-1}$ at 1σ . Note that this constraint is independent of the value of the Barbero-Immirzi parameter and should be valid for any value for γ . Using Eq. (5.8), it translates into a lower limit on N_T depending on the value for the Barbero-Immirzi parameter, which is described by

$$N_T \gtrsim 139 - \frac{3}{2} \ln(\gamma). \quad (5.9)$$

Note that N_T can be expressed as

$$\begin{aligned} N_T &= \ln \left(\frac{a_0}{a_B} \right) = \ln \left(\frac{a_i}{a_B} \frac{a_{\text{end}}}{a_i} \frac{a_{\text{reh}}}{a_{\text{end}}} \frac{a_0}{a_{\text{reh}}} \right) \\ &= N_{\text{pre}} + N_{\text{infl}} + N_{\text{reh}} + \ln \left(\frac{a_0}{a_{\text{reh}}} \right), \end{aligned} \quad (5.10)$$

where a_i , a_{end} and a_{reh} are the scale factors at the beginning of inflation, at the end of inflation and at the end of the reheating phase, respectively, while N_{reh} is the duration of the reheating phase. We also have that [67]

$$\frac{a_0}{a_{\text{reh}}} = \left(\frac{11g_{s,\text{reh}}}{43} \right)^{\frac{1}{3}} \frac{T_{\text{reh}}}{T_{\text{CMB},0}}, \quad (5.11)$$

where T_{reh} is the reheating temperature, $T_{\text{CMB},0}$ is the temperature of the CMB today and $g_{s,\text{reh}}$ is the effective number of relativistic degrees of freedom for entropy at the end of reheating. Considering the case of instantaneous reheating at the end of inflation (i.e., neglecting the typically unknown physics at reheating), $N_{\text{reh}} \approx 0$ and we can associate T_{reh} with the inflaton potential energy density at the end of inflation, V_{end} , as

$$T_{\text{reh}} \simeq \left(\frac{30}{g_{\text{reh}}\pi^2} \right)^{\frac{1}{4}} (1 + \kappa)^{\frac{1}{4}} V_{\text{end}}^{\frac{1}{4}}, \quad (5.12)$$

where g_{reh} is the effective number of relativistic degrees of freedom for energy at full thermalization. In Eq. (5.12), κ is the ratio of kinetic energy to potential energy during inflation. At the end of inflation, $\kappa = 1/2$. By taking both $g_{s,\text{reh}}$ and g_{reh} to be close to those for the standard model of particle physics, $g_{s,\text{reh}} \simeq g_{\text{reh}} \sim 100$, we obtain that $\ln(a_0/a_{\text{reh}}) \sim 60$. Thus, Eq. (5.9) can also be written as a lower bound for $N_{\text{pre}} + N_{\text{infl}}$,

$$N_{\text{pre}} + N_{\text{infl}} \gtrsim 79 - \frac{3}{2} \ln(\gamma). \quad (5.13)$$

Adding the reheating details after inflation only makes the above relation more restrictive. Thus, we can use Eq. (5.13) as an overall lower bound for the total number of e -folds from the bounce until the end of inflation as a function of the Barbero-Immirzi parameter. By considering the value for γ as given by the value suggested by the black hole entropy [55], $\gamma \simeq 0.2375$, we then obtain that $N_T \gtrsim 141$ and $N_{\text{pre}} + N_{\text{infl}} \gtrsim 81$. Recalling also that the number of e -folds relevant from the CMB observations (e.g., at a pivot scale $k_* = 0.05/\text{Mpc}$ and

assuming instant reheating for simplicity) is given by [4]

$$N_* \approx 57 + 2 \ln \left(\frac{V_*^{1/4}}{10^{16} \text{ GeV}} \right) - \ln \left(\frac{T_{\text{reh}}}{10^{16} \text{ GeV}} \right), \quad (5.14)$$

which typically leads to $N_* \sim 50 - 60$ for the necessary number of e -folds of inflation. As we have seen that $N_{\text{pre}} \sim 4$, which is very weakly dependent on the form of the inflaton potential, then N_* can comfortably fit in the estimated lower bound $N_{\text{pre}} + N_{\text{infl}} \gtrsim 81$.

In the following we analyze the general behavior of the number of e -folds $N_{\text{pre+infl}} = N_{\text{pre}} + N_{\text{infl}}$ lasting from the bounce until the end of inflation, as a function of γ . The general expressions for N_{pre} and N_{infl} were derived in the previous section. Next, we will consider how $N_{\text{pre+infl}}$ changes by varying the Barbero-Immirzi parameter and also by considering the overall lower bound given by Eq. (5.13).

C. Results for the Barbero-Immirzi parameter

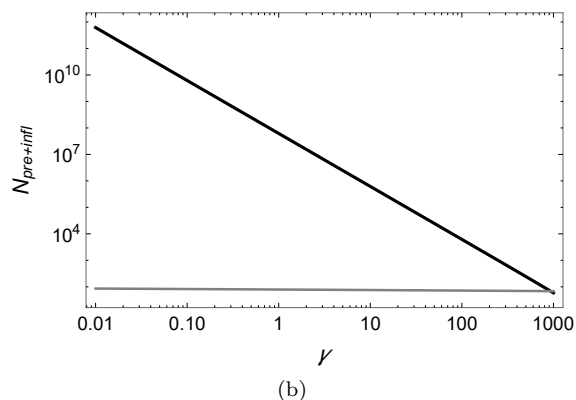
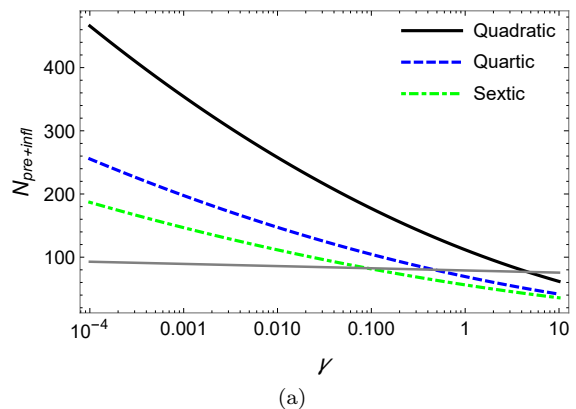


FIG. 4. Number of preinflationary plus inflationary e -folds, $N_{\text{pre+infl}}$, for the potentials considered, varying the Barbero-Immirzi parameter. The almost horizontal gray lines show the lower limit on $N_{\text{pre+infl}}(\gamma)$ set by Eq. (5.13). Panel (a): power-law potentials; panel(b): Starobinsky potential.

The behavior of the number of e -folds from the bounce

to the end of inflation as a function of γ for each potential considered in this paper is shown in Figs. 4 and 5. We show in Fig. 4(a) the case of monomial power-law potentials. We consider a sufficiently long range of representative values for γ (the range $0 \lesssim \gamma \lesssim 10$ typically corresponds to the interval most considered in the literature [41–45]). The almost horizontal gray lines in Figs. 4 and 5 show the lower limit on $N_{\text{pre+infl}}(\gamma)$ set by Eq. (5.13). In all cases it is observed that the smaller the value of γ , the greater the value of $N_{\text{pre+infl}}$. For the quadratic case ($n = 1$) we obtain a value of $N_{\text{pre+infl}}$ which satisfies the observational constraints for almost the entire interval of γ . However, the quartic ($n = 2$) and sextic ($n = 3$) cases approach the limit of 81 e -folds for smaller values of γ . For the quartic case ($n = 2$), we get that for $\gamma \sim 0.46$, $N_{\text{pre+infl}}$ reaches the value of 81 e -folds. For the sextic case ($n = 3$), we get that for $\gamma \sim 0.1$, the number of e -folds reaches the limiting value $N_{\text{pre+infl}} = 81$ and quickly drops below this value as γ increases. We can see that, although for the usual value of the Barbero-Immirzi parameter the sextic potential in LQC is in strong tension with the observations, for smaller values of the parameter, $\gamma < 0.1$, it can be consistent.

Complementing these results, we show in Fig. 4(b) the results for the number of e -folds as a function of γ for the Starobinsky potential. We can see that, again, this corresponds to the case that presents the highest values for $N_{\text{pre+infl}}$.⁹ We analyzed what value for the γ parameter would lead to the limiting value of $N_{\text{pre+infl}} = 81$. The numerical results shows that in this case the value of the Barbero-Immirzi parameter would be around $\gamma \sim 1000$, as can be seen in Fig. 4(b). Note that although γ is typically expected to be approximately of order 1, a large γ is not inconsistent.

To complete our analysis, the results for the Higgs-like potential is shown in Fig. 5. The number of e -folds as a function of γ for the large field case is shown in Fig. 5(a), while for the small field case it is shown in Fig. 5(b). In both cases, representative values for the VEV are considered. We observe from Fig. 5(a), which is for the large field case, that $N_{\text{pre+infl}}$ decreases when γ increases. For all VEVs considered, we observe a similar behavior and we see that the limit $N_{\text{pre+infl}} = 81$ occurs when $\gamma \approx 1.15$. On the other hand, for the small field case, shown in Fig. 5(b), it is possible to observe that the higher the VEV, the higher the number of e -folds for each value of γ , up to some critical value for γ , above which the number of e -folds decreases. The decreasing behavior for the number of e -folds seen here, and that happens above some value of γ , is a consequence of the effect already discussed in connection to the one seen in Fig. 3(b). Increasing γ changes the point (VEV) where

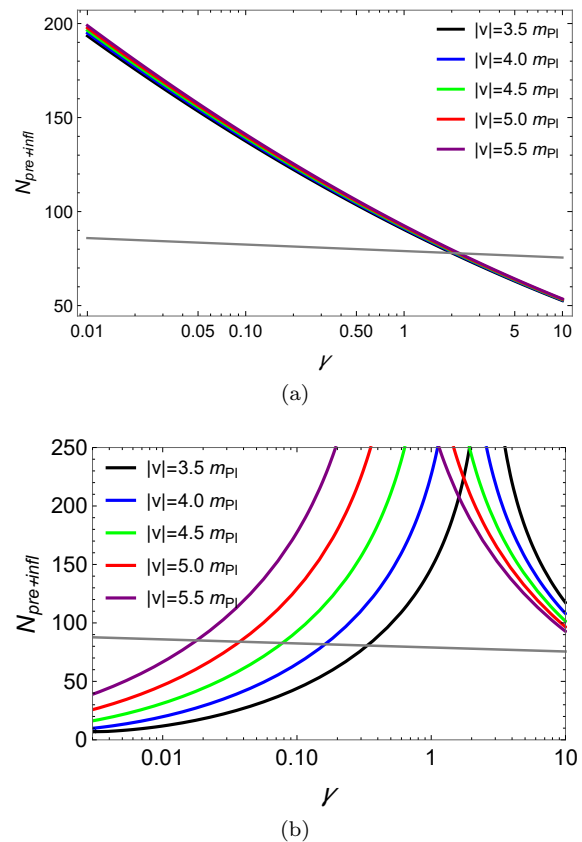


FIG. 5. Number of e -folds, $N_{\text{pre+infl}}$, as a function of the Barbero-Immirzi parameter for the Higgs-like potential with different values of the VEV. The almost horizontal gray lines show the lower limit on $N_{\text{pre+infl}}(\gamma)$ set by Eq. (5.13). Panel (a): the results for the large field case $|\phi| > |v|$. Panel (b): the results for the small field case $|\phi| < |v|$.

the number of e -folds peaks when inflation happens in the plateau region of the potential. For VEVs larger than around $7m_{\text{Pl}}$, the number of e -folds drops below the lower bound set by Eq. (5.13) for $\gamma \sim 10$, but for even higher VEVs, the lower bound will be reached for much smaller values of γ .

The results given above show that for different values of γ the predictions for observational signals of LQC in CMB are considerably different. We see that the consistency of the models with the current data depends strongly on the value of this parameter. This motivates and highlights the importance of a careful analysis of the role of the Barbero-Immirzi parameter in these scenarios.

VI. CONCLUSIONS

It is well known that the primordial power spectrum is a quantity that can relate the theory of the early Universe with the observations. Previous works in the literature have shown that the predictions for the power spectrum in the context of LQC receive a correction term with re-

⁹ See, for example, Ref. [37] for an analysis on the duration of the slow-roll inflation for this kind of potential in the presence of shear.

spect to the predictions in the context of GR. As shown in Ref. [10], due to this correction term, models in the context of LQC require a minimum amount of ~ 81 e -folds of expansion from the bounce until the end of the slow-roll inflationary phase in order to be consistent with the observations. However, the prediction for the duration of inflation in LQC depends on how the initial conditions for the dynamics are set.

A previous work [30] investigated in detail the duration of inflation for LQC models with monomial and Higgs-like potentials and which was considered initial conditions far in the contracting phase, thus well before the bounce (extending the analysis made in Refs. [10, 11, 24, 26, 33–38]). In the present paper, we have investigated the duration of inflation in these same models, including also the Starobinsky potential, but now from a different perspective concerning the initial conditions. As discussed, the dynamics in the LQC models considered here starts in the contracting phase sufficiently before the bounce, such that the kinetic energy of the inflaton field necessarily comes to dominate at the bounce. Then, we have shown that it is possible to estimate the inflaton field amplitude at some intermediate instant in the contracting phase, but still well before the bounce. With that value for the inflaton amplitude, we can forward the background dynamics up to the bounce instant and determine the value for the inflaton field at that instant, ϕ_B . With ϕ_B uniquely determined, all subsequent background dynamics from the bounce until the end of inflation can then be determined. In LQC models in which the evolution of the inflaton field is dominated by its kinetic energy at the quantum bounce, a slow-roll inflation phase is practically always reached as is also demonstrated by our results. With the initial conditions taken deeper in the contracting phase, the kinetic energy regime dominates earlier and longer until the bounce is reached. Hence, we expect the results to turn out to be weakly dependent on the inflationary potential, as our results indicate. This also implies that the results turn out to be weakly dependent on the specific value adopted for the ratio of the kinetic and potential energy.

For all the models analyzed, we found that the number of e -folds of the preinflationary phase is approximately $N_{\text{pre}} \sim 4$. On the other hand, the number of inflationary e -folds changes considerably depending on the potential for the inflaton. Monomial potentials like $V \propto |\phi|^5$ and with higher powers tend to predict a too small value for the number of inflationary e -folds and, thus, they are likely to be incompatible with the CMB data. The quartic potential, $V \propto \phi^4$, on the other hand, predicts the most likely N_{inff} to be around $N_{\text{inff}} \sim 86$, which suggests a very good possibility of leading to observable signatures from LQC in the spectrum of CMB data. For the quadratic model, $V \propto \phi^2$, the most likely N_{inff} is around $N_{\text{inff}} \sim 147$. This is in agreement with the results obtained in the earlier work done in Ref. [34]. With such high values of N_{inff} allowed by the quadratic potential, the effects from the quantum regime would probably

be diluted to an unobservable level. For the Higgs-like symmetry-breaking potential we have shown that N_{inff} grows with the VEV v for the case of inflation occurring in the plateau (small-field) region. It reaches a maximum value for the number of e -folds at a VEV around $v \sim 5m_{\text{Pl}}$ and beyond this value N_{inff} drops and tends to asymptote at around $N_{\text{inff}} \sim 200$. For inflation occurring in the large-field ($|\phi| > |v|$) part of the potential N_{inff} has a weak dependence on v , being around $N_{\text{inff}} \sim 110$ in the range of values of v we have considered. Even though these results were obtained for a Higgs-like potential, we expect the features displayed would also be present in other small field types of potentials, like hilltop and axionlike potentials. For the Starobinsky model, we predict a much higher value for N_{inff} when compared to the other potentials studied, with $N_{\text{inff}} \sim 10^9$. This implies no potentially observable signal that could be searched for on CMB data as far as the Starobinsky model is considered in the context of LQC.

We have also shown in the present paper that the value of the Barbero-Immirzi parameter can affect strongly the constraints on the number of e -folds. The Barbero-Immirzi parameter is strictly a free parameter of the underlying LQG theory. Being related to the typical scale at the bounce, the Barbero-Immirzi parameter implies in different predictions for the power spectrum in LQC. In fact, what CMB actually constrains is the combination of the parameters γ and $N_{\text{pre+inff}}$, the total number of e -folds from the bounce until the end of inflation. Therefore, it is important to investigate the relation between the predictions for the number of e -folds in LQC with the value of γ . This analysis is performed in detail, for the first time, in the present paper.

The results presented in this paper show that for different values of γ the predictions for the duration of inflation in LQC are considerably different. For the monomial potentials, the predicted number of e -folds decreases with the value of γ . In particular it is interesting to see that, for example in the case of the sextic potential in LQC, although for the usual value of the Barbero-Immirzi parameter the model is in strong tension with the observations, for smaller values of the parameter, like $\gamma \lesssim 0.1$, it can be consistent with the increase of the predicted number of e -folds when γ is lower than the usual value adopted for it in the literature. For the Higgs-like potential, we have obtained that the number of e -folds increases with γ in the small field case, up to some critical value, beyond which, with the increase of γ , it starts to decrease. For the large field case, on the other hand, the number of e -folds always decreases when γ increases. For the Starobinsky model, we have obtained that the prediction for the number of e -folds decreases with γ . The number of e -folds can reach the limiting value of $N \simeq 81$ for the value of the Barbero-Immirzi parameter $\gamma \sim 1000$, which is, nevertheless, a quite high value to be acceptable by the underlying LQG theory.

It is important to remark that the observable predictions in LQC and the constraints obtained for the

Barbero-Immirzi parameter are dependent on the way initial conditions are set. In this work we considered the initial conditions for the perturbations to be the BD vacuum in the contracting phase in the context of the dressed metric approach, which leads to basically the same results as considering the fourth-order adiabatic vacuum state at the bounce in the context of the dressed metric approach. We obtain that the observable predictions in LQC models are dependent also on the value of the Barbero-Immirzi parameter, being quite sensitive to the latter. We obtain limits for γ directly from the primordial scalar power spectrum. Since the consistency of the models with the current data depends strongly on the value of this parameter, this paper highlights for the first time the importance of a careful analysis of the role of the Barbero-Immirzi parameter in LQC.

Finally, in this paper we have analyzed only the case of a Universe with energy density made essentially of the inflaton field. As possible follow-ups of this paper, it would be interesting to perform a similar analysis when other energy contents are present, like from sources of anisotropies [35, 37] or when radiation is also present, which itself has been shown to lead to interesting results in the context of LQC [29, 30, 53, 68–71].

VII. ACKNOWLEDGMENTS

L.N.B. acknowledges financial support of the Coordenação de Aperfeiçoamento de Pessoal de Nível Superior (CAPES) - Finance Code No. 001. G.L.L.W.L. acknowledges financial support of the Conselho Nacional de Desenvolvimento Científico e Tecnológico (CNPq). L.L.G is supported by CNPq, under the Grant No. 307052/2019-2, and by the Fundação Carlos Chagas Filho de Amparo à Pesquisa do Estado do Rio de Janeiro (FAPERJ), Grant No. E-26/201.297/2021. R.O.R. is partially supported by research grants from CNPq, Grant No. 307286/2021-5, and from FAPERJ, Grant No. E-26/201.150/2021. R.O.R. also acknowledges financial support of the Coordenação de Aperfeiçoamento de Pessoal de Nível Superior (CAPES) - Finance Code No. 001. One of us (L.L.G.) wishes to thank the Kavli Institute for the Physics and Mathematics of the Universe (IPMU) for kind hospitality.

Appendix A: Obtaining V_0 through the CMB spectrum

Let us now briefly review the derivation of the normalization V_0 for each of the potentials we have considered in this paper. The primordial scalar curvature power spectrum $\Delta_{\mathcal{R}}$ is given by the standard expression [56]

$$\Delta_{\mathcal{R}} = \left(\frac{H_*^2}{2\pi\dot{\phi}_*} \right)^2, \quad (\text{A1})$$

where a subindex $*$ means that the quantities are evaluated at the Hubble radius crossing k_* ($k_* = a_* H_*$). This is typically assumed to happen around $N_* \sim 50 - 60$ e -folds before the end of inflation. In this work we have assumed the fiducial value of 60 e -folds for illustration purposes. The value of V_0 is fixed by the normalization of the primordial scalar of curvature power spectrum. The Planck collaboration [72] gives for instance the value $\ln(10^{10}\Delta_{\mathcal{R}}) \simeq 3.047$ (TT,TE,EE-lowE+lensing+BAO 68% limits). This is the value we have adopted in this paper to obtain the normalization V_0 .

During the slow-roll regime of inflation, we can make the approximations $H^2 \simeq 8\pi V/(3m_{\text{Pl}}^2)$ and $\dot{\phi} \simeq -V_{,\phi}/(3H)$. Thus,

$$\Delta_{\text{R}} \simeq \frac{128\pi}{3} \frac{V_*^3}{m_{\text{Pl}}^6 V_{,\phi_*}^2}, \quad (\text{A2})$$

for any given potential.

For the monomial power-law potentials [Eq. (2.6)], Eq. (A2) gives

$$\Delta_{\text{R}} = \frac{4}{3(4\pi)^n} \frac{1}{n^3} \frac{V_0^{\text{mon}}}{m_{\text{Pl}}^4} [n(2N_* + n)]^{n+1}, \quad (\text{A3})$$

where we have used that

$$\phi_* \equiv \phi(N_*) = \sqrt{(nm_{\text{Pl}}^2/4\pi)(2N_* + n)}. \quad (\text{A4})$$

Therefore, the normalization V_0 obtained from CMB measurements gives

$$\frac{V_0^{\text{mon}}}{m_{\text{Pl}}^4} = \frac{3(4\pi)^n}{4} \frac{n^3}{[n(2N_* + n)]^{n+1}} \Delta_{\text{R}}. \quad (\text{A5})$$

For the Higgs-like potential (2.7), we find, analogously, that

$$\Delta_{\text{R}} = \frac{2\pi}{3m_{\text{Pl}}^6} \frac{V_0^{\text{Higgs}}}{m_{\text{Pl}}^4} \frac{(\phi_*^2 - v^2)^4}{\phi_*^2}. \quad (\text{A6})$$

Solving for V_0 , we find

$$\frac{V_0^{\text{Higgs}}}{m_{\text{Pl}}^4} = \frac{3m_{\text{Pl}}^6}{2\pi} \Delta_{\text{R}} \frac{\phi^2(N_*)}{[\phi_i^2(N_*) - v^2]^4}, \quad (\text{A7})$$

where $\phi(N_*)$ is obtained from the expression (3.27), which gives two possible solutions,

$$\phi^2(N_*) = -v^2 W_0 \left[-\frac{\phi_{\text{end}}^2}{v^2} \left(e^{\frac{N_* + \phi_{\text{end}}^2}{\pi} + \frac{\phi_{\text{end}}^2}{m_{\text{Pl}}^2}} \right)^{-\frac{m_{\text{Pl}}^2}{v^2}} \right] \quad (\text{A8})$$

and

$$\phi^2(N_*) = -v^2 W_{-1} \left[-\frac{\phi_{\text{end}}^2}{v^2} \left(e^{\frac{N_* + \phi_{\text{end}}^2}{\pi} + \frac{\phi_{\text{end}}^2}{m_{\text{Pl}}^2}} \right)^{-\frac{m_{\text{Pl}}^2}{v^2}} \right], \quad (\text{A9})$$

where W_0 and W_{-1} correspond to the Lambert functions and ϕ_{end} is given by Eq. (3.28). It can be verified that the solution given by Eq. (A8) applies when inflation happens in the small field region of the potential, i.e., around the plateau region, $|\phi| < |v|$. The second solution given by Eq. (A9), on the other hand, applies in the large field region of the potential, i.e., when $|\phi| > |v|$.

For the Starobinsky potential, Eq. (2.8), the normal-

ization V_0 is found to be

$$\frac{V_0^{\text{Staro}}}{m_{\text{Pl}}^4} = \frac{e^{-8\sqrt{\frac{\pi}{3}}\frac{\phi_*}{m_{\text{Pl}}}}}{2\left(1 - e^{-4\sqrt{\frac{\pi}{3}}\frac{\phi_*}{m_{\text{Pl}}}}\right)^4} \Delta_{\text{R}}, \quad (\text{A10})$$

where ϕ_* is given by

$$\phi(N_*) = -\frac{m_{\text{Pl}}}{4\sqrt{3}\pi} \left\{ 4N_* + 3 + 2\sqrt{3} + \ln\left(-135 + 78\sqrt{3}\right) + 3W_{-1}\left[-\left(1 + \frac{2}{\sqrt{3}}\right)e^{-\frac{4N_*}{3} - 1 - \frac{2}{\sqrt{3}}}\right] \right\}. \quad (\text{A11})$$

-
- [1] A. D. Linde, Inflationary cosmology, Lect. Notes Phys. **738**, 1 (2008).
- [2] J. A. Vázquez, L. E. Padilla, and T. Matos, Inflationary cosmology: From theory to observations, Rev. Mex. Fis. E **17**, 73 (2020).
- [3] L. Kofman, A. D. Linde, and V. F. Mukhanov, Inflationary theory and alternative cosmology, J. High Energy Phys. **10** (2002) 057.
- [4] Y. Akrami *et al.* (Planck Collaboration), Planck 2018 results. X. Constraints on inflation, Astron. Astrophys. **641**, A10 (2020).
- [5] A. Borde and A. Vilenkin, Eternal Inflation and the Initial Singularity, Phys. Rev. Lett. **72**, 3305 (1994).
- [6] A. Borde, A. H. Guth, and A. Vilenkin, Inflationary Space-Times are Incomplete in Past Directions, Phys. Rev. Lett. **90**, 151301 (2003).
- [7] J. Martin, C. Ringeval, and V. Vennin, Encyclopædia inflationaris, Phys. Dark Universe. **5-6**, 75 (2014).
- [8] R. Brandenberger and X. m. Zhang, The trans-Planckian problem for inflationary cosmology revisited, arXiv:0903.2065.
- [9] R. H. Brandenberger and J. Martin, Trans-Planckian issues for inflationary cosmology, Classical Quantum Gravity. **30**, 113001 (2013).
- [10] T. Zhu, A. Wang, G. Cleaver, K. Kirsten, and Q. Sheng, Pre-inflationary universe in loop quantum cosmology, Phys. Rev. D **96**, 083520 (2017).
- [11] M. Shahalam, M. Sharma, Q. Wu, and A. Wang, Pre-inflationary dynamics in loop quantum cosmology: Power-law potentials, Phys. Rev. D **96**, 123533 (2017).
- [12] M. Shahalam, K. Yesmakhanova, and Z. Umurzakhova, Initial conditions of pre-inflation with Hilltop potential in loop quantum cosmology, arXiv:2108.06218.
- [13] M. Martín-Benito, R. B. Neves, and J. Olmedo, States of low energy in bouncing inflationary scenarios in loop quantum cosmology, Phys. Rev. D **103**, 123524 (2021).
- [14] A. Ashtekar and P. Singh, Loop quantum cosmology: A status report, Classical Quantum Gravity **28**, 213001 (2011).
- [15] A. Barrau, T. Cailleteau, J. Grain, and J. Mielczarek, Observational issues in loop quantum cosmology, Classical Quantum Gravity **31**, 053001 (2014).
- [16] I. Agullo and P. Singh, *Loop Quantum Cosmology* (World Scientific, Singapore, 2017).
- [17] M. Bojowald, Loop quantum cosmology, Living Rev. Relativity **8**, 11 (2005).
- [18] A. Ashtekar, M. Bojowald, and J. Lewandowski, Mathematical structure of loop quantum cosmology, Adv. Theor. Math. Phys. **7**, 233 (2003).
- [19] A. Ashtekar, T. Pawłowski, and P. Singh, Quantum Nature of the Big Bang, Phys. Rev. Lett. **96**, 141301 (2006).
- [20] A. Ashtekar and D. Sloan, Loop quantum cosmology and slow roll inflation, Phys. Lett. B **694**, 108 (2011).
- [21] B. Elizaga Navascués and G. A. M. Marugán, Hybrid loop quantum cosmology: An overview, Front. Astron. Space Sci. **8**, 81 (2021).
- [22] K. Banerjee, G. Calcagni, and M. Martin-Benito, Introduction to loop quantum cosmology, SIGMA **8**, 016 (2012).
- [23] B. F. Li, P. Singh, and A. Wang, Qualitative dynamics and inflationary attractors in loop cosmology, Phys. Rev. D **98**, 066016 (2018).
- [24] M. Sharma, M. Shahalam, Q. Wu, and A. Wang, Pre-inflationary dynamics in loop quantum cosmology: Monodromy potential, J. Cosmol. Astropart. Phys. **11** (2018) 003.
- [25] B. F. Li, P. Singh, and A. Wang, Genericness of pre-inflationary dynamics and probability of the desired slow-roll inflation in modified loop quantum cosmologies, Phys. Rev. D **100**, 063513 (2019).
- [26] M. Shahalam, M. Al Ajmi, R. Myrzakulov, and A. Wang, Revisiting pre-inflationary universe of family of α -attractor in loop quantum cosmology, Classical Quantum Gravity **37**, 195026 (2020).
- [27] A. Barrau, A pure general relativistic non-singular bouncing origin for the Universe, Eur. Phys. J. C **80**, 579 (2020).
- [28] S. Bedić and G. Vereshchagin, Probability of inflation in loop quantum cosmology, Phys. Rev. D **99**, 043512 (2019).
- [29] L. L. Graef and R. O. Ramos, Probability of warm inflation in loop quantum cosmology, Phys. Rev. D **98**, 023531 (2018).
- [30] L. N. Barboza, L. L. Graef, and R. O. Ramos, Warm bounce in loop quantum cosmology and the prediction for the duration of inflation, Phys. Rev. D **102**, 103521 (2020).
- [31] A. H. Guth, The inflationary universe: A possible solution to the horizon and flatness problems, Phys. Rev. D **23**, 347 (1981).
- [32] I. Agullo, A. Ashtekar, and W. Nelson, The pre-inflationary dynamics of loop quantum cosmology: Con-

- fronting quantum gravity with observations, *Classical Quantum Gravity* **30**, 085014 (2013).
- [33] A. Ashtekar and D. Sloan, Probability of inflation in loop quantum cosmology, *Gen. Relativ. Gravit.* **43**, 3619 (2011).
- [34] L. Linsefors and A. Barrau, Duration of inflation and conditions at the bounce as a prediction of effective isotropic loop quantum cosmology, *Phys. Rev. D* **87**, 123509 (2013).
- [35] L. Linsefors and A. Barrau, Exhaustive investigation of the duration of inflation in effective anisotropic loop quantum cosmology, *Classical Quantum Gravity* **32**, 035010 (2015).
- [36] B. Bolliet, A. Barrau, K. Martineau, and F. Moulin, Some clarifications on the duration of inflation in loop quantum cosmology, *Classical Quantum Gravity* **34**, 145003 (2017).
- [37] K. Martineau, A. Barrau, and S. Schander, Detailed investigation of the duration of inflation in loop quantum cosmology for a Bianchi-I universe with different inflation potentials and initial conditions, *Phys. Rev. D* **95**, 083507 (2017).
- [38] L. Chen and J. Y. Zhu, Loop quantum cosmology: The horizon problem and the probability of inflation, *Phys. Rev. D* **92**, 084063 (2015).
- [39] A. Barrau, K. Martineau, and F. Moulin, A status report on the phenomenology of black holes in loop quantum gravity: Evaporation, tunneling to white holes, dark matter and gravitational waves, *Universe* **4**, 102 (2018).
- [40] J. Armas and J. Armas, *Conversations on Quantum Gravity* (Cambridge University Press, Cambridge, England, 2021), ISBN 978-1-316-71763-9, 978-1-107-16887-9.
- [41] S. K. Asante, B. Dittrich, and H. M. Haggard, Effective Spin Foam Models for Four-Dimensional Quantum Gravity, *Phys. Rev. Lett.* **125**, 231301 (2020).
- [42] S. K. Asante, B. Dittrich, and J. Padua-Arguelles, Effective spin foam models for Lorentzian quantum gravity, *Classical Quantum Gravity* **38**, 195002 (2021).
- [43] L. Perlov, Barbero-Immirzi value from experiment, *Mod. Phys. Lett. A* **36**, 2150192 (2021).
- [44] B. Broda and M. Szanecki, A relation between the Barbero-Immirzi parameter and the standard model, *Phys. Lett. B* **690**, 87 (2010).
- [45] S. Mercuri and V. Taveras, Interaction of the Barbero-Immirzi field with matter and pseudoscalar perturbations, *Phys. Rev. D* **80**, 104007 (2009).
- [46] S. J. Gates, Jr., S. V. Ketov, and N. Yunes, Seeking the loop quantum gravity Barbero-Immirzi parameter and field in 4D, $N = 1$ supergravity, *Phys. Rev. D* **80**, 065003 (2009).
- [47] S. Boudet, F. Bombacigno, G. Montani, and M. Rinaldi, Superentropic black hole with Immirzi hair, *Phys. Rev. D* **103**, 084034 (2021).
- [48] C. Pigozzo, F. S. Bacelar, and S. Carneiro, On the value of the Immirzi parameter and the horizon entropy, *Classical Quantum Gravity* **38**, 045001 (2021).
- [49] S. Carneiro and C. Pigozzo, Quasinormal modes and horizon area quantization in loop quantum gravity, *Gen. Relativ. Gravit.* **54**, 20 (2022); **54**, 25(E) (2022).
- [50] J. Engle, K. Noui, A. Perez, and D. Pranzetti, Black hole entropy from an $SU(2)$ -invariant formulation of type I isolated horizons, *Phys. Rev. D* **82**, 044050 (2010).
- [51] E. Bianchi, Entropy of nonextremal black holes from loop gravity, arXiv:1204.5122.
- [52] P. J. Wong, Shape dynamical loop gravity from a conformal Immirzi parameter, *Int. J. Mod. Phys. D* **26**, 1750131 (2017).
- [53] M. Benetti, L. Graef, and R. O. Ramos, Observational constraints on warm inflation in loop quantum cosmology, *J. Cosmol. Astropart. Phys.* **10** (2019) 066.
- [54] M. Benetti and R. O. Ramos, Warm inflation dissipative effects: Predictions and constraints from the Planck data, *Phys. Rev. D* **95**, 023517 (2017).
- [55] K. A. Meissner, Black hole entropy in loop quantum gravity, *Classical Quantum Gravity* **21**, 5245 (2004).
- [56] D. H. Lyth and A. R. Liddle, *The Primordial Density Perturbation: Cosmology, Inflation and the Origin of Structure*, (Cambridge University Press, Cambridge, England, 2009).
- [57] P. A. R. Ade *et al.* (BICEP and Keck Collaborations), Improved Constraints on Primordial Gravitational Waves using Planck, WMAP, and BICEP/Keck Observations through the 2018 Observing Season, *Phys. Rev. Lett.* **127**, 151301 (2021).
- [58] A. A. Starobinsky, A new type of isotropic cosmological models without singularity, *Phys. Lett.* **91B**, 99 (1980).
- [59] M. S. Turner, Coherent scalar field oscillations in an expanding universe, *Phys. Rev. D* **28**, 1243 (1983).
- [60] M. Bastero-Gil, A. Berera, R. Brandenberger, I. G. Moss, R. O. Ramos, and J. G. Rosa, The role of fluctuation-dissipation dynamics in setting initial conditions for inflation, *J. Cosmol. Astropart. Phys.* **01** (2018) 002.
- [61] M. Cicoli, C. P. Burgess, and F. Quevedo, Fibre inflation: Observable gravity waves from IIB string compactifications, *J. Cosmol. Astropart. Phys.* **03** (2009) 013.
- [62] I. Agullo, A. Ashtekar, and W. Nelson, A Quantum Gravity Extension of the Inflationary Scenario, *Phys. Rev. Lett.* **109**, 251301 (2012).
- [63] M. Fernandez-Mendez, G. A. Mena Marugan, and J. Olmedo, Hybrid quantization of an inflationary universe, *Phys. Rev. D* **86**, 024003 (2012).
- [64] B. F. Li, J. Olmedo, P. Singh, and A. Wang, Primordial scalar power spectrum from the hybrid approach in loop cosmologies, *Phys. Rev. D* **102**, 126025 (2020).
- [65] B. F. Li, T. Zhu, A. Wang, K. Kirsten, G. Cleaver, and Q. Sheng, Preinflationary perturbations from the closed algebra approach in loop quantum cosmology, *Phys. Rev. D* **99**, 103536 (2019).
- [66] G. S. Vicente, R. O. Ramos, and L. L. Graef, Gravitational particle production and the validity of effective descriptions in loop quantum cosmology, *Phys. Rev. D* **106**, 043518 (2022).
- [67] J. B. Munoz and M. Kamionkowski, Equation-of-state parameter for reheating, *Phys. Rev. D* **91**, 043521 (2015).
- [68] R. Herrera, Warm inflationary model in loop quantum cosmology, *Phys. Rev. D* **81**, 123511 (2010).
- [69] K. Xiao and J. Y. Zhu, A phenomenology analysis of the tachyon warm inflation in loop quantum cosmology, *Phys. Lett. B* **699**, 217 (2011).
- [70] X. M. Zhang and J. Y. Zhu, Warm inflation in loop quantum cosmology: A model with a general dissipative coefficient, *Phys. Rev. D* **87**, 043522 (2013).
- [71] K. Xiao and S. Q. Wang, Pre-inflation dynamical behavior of warm inflation in loop quantum cosmology, *Mod. Phys. Lett. A* **35**, 2050293 (2020).
- [72] N. Aghanim *et al.* (Planck Collaboration), Planck 2018 results. VI. Cosmological parameters, *Astron. Astrophys.* **641**, A6 (2020); **652**, C4(E) (2021).